In-vitro Study of Cartilage Differentiation of Enthesis Tissue Engineering

A Thesis submitted in partial fulfillment of the requirements for the degree of

Master of Technology

In

BIOTECHNOLOGY

By

VINAY KUMAR

212BM2027

Under The Supervision of

Prof. B.P. NAYAK

Department of Biotechnology & Medical Engineering

National Institute of Technology

Rourkela-769008, Orissa, India

May, 2015

Department of Biotechnology & Medical Engineering,
National Institute of Technology, Rourkela
Odisha 769008

Certificate

This is to certify that the report entitled, "**In-vitro Study of Cartilage Differentiation for Enthesis Tissue Engineering**", submitted by **Vinay Kumar**, Roll No.: **212BM2027**, M.Tech-4th semester, Department of Biotechnology & Medical Engineering, National Institute of Technology, Rourkela (Deemed University) is an authentic work carried out by her under my supervision and guidance.

To the best of my knowledge, the matter embodied in the report has not been submitted to any other University / Institute for the award of any Degree or Diploma.

Date:

Dr. B. P. NAYAK

Department of Biotechnology & Medical Engineering

National Institute of Technology

Rourkela – 769008

ACKNOWLEDGEMENT

I express my deep sense of gratitude and indebtness to **Dr.B.P.Nayak**, my research guide, who apart from dedicating an important part of his time, has provided me with a logistic vision to conduct experiments and concentrate on important matters. I am very lucky being one of his students. He has been a source of inspiration to learn and understand the subject more deeply, I am very thankful for his sincere support and constant encouragement. I am very grateful to **Mr. Rakesh Buhlan, Mr. Joseph Christakiran M**., **Mr.Gautham Hari Narayana, Ms. AnuPriya, Ms. Trupti Patil**, for the informative discussions and creating a healthy workplace environment in lab. Finally I would like to thank all the staff of NITR for their support and valuable suggestions during my project work. I would also like to extend my deep gratitude to **Mr. Patitapabana Parida**, Research Associate for his help and ensuring that all the instruments are producing proper results and there was never a shortage of reagents and chemicals. This project work would not have seen this day of completion had there not been a constant support and encouragement from my family and friends. I am deeply thankful to them.

Vinay Kumar

CONTENTS

LIST OF FIGURES

ABSTRACT

Ligaments are a dense connective tissue responsible for joint movements and stability. Anterior Cruciate Ligament (ACL) is one of the four major ligaments of the knee which is protruding out from the notch of the femur leads back into the femoral chondyle and fixes deep within tibia of the lower Limb. Being subjected to high physiological loads, ACL is commonly injured and failed to heal optimally due to its low cellularity and vascularity. Surgical management with ligament grafts is often required, but these treatments are associated with complications of reduced strength, joint stiffness, repair-rupture, as well as donor-site morbidity. Interface Tissue engineering (ITE) may effectively address these complications where an artificial ligament incorporating the interfacial fibrocartilage can be engineered to provide similar mechanical and functional characteristics as the native tissue. Therefore a multi-compartmental scaffold that can induce the growth and differentiation of fibrocartilage at the interface of engineered bone and ligament tissues would mimic the native structure of bone-ligament –bone block with deposition of appropriate extracellular matrix (ECM) in respective compartments and possession of adequate mechanical properties to support the healing tissue. The current project has focused on the fabrication of a silk-based knitted scaffold which comprises of three compartments, one each for the bone, ligament and enthesis tissues. an array of methods were adopted for surface modification of the compartmentalized knitted silk scaffold by using bio-polymers such as silk solution, chitosan, gelatin and hydroxyapatite on the appropriate compartments. The ligament and bone compartments were reserved for mature cell line culture like MG63 and Saos-2. The various methods used for coatings of polymers over the knitted-silk were alternate soaking, plain coating and freeze-drying. The knitted scaffold was characterized for its water absorption biodegradability, tensile strength, and biocompatibility. After coated with the polymers the tensile strength of knitted scaffold is increased by 33% compare to without coating.It was concluded that the multi-compartment silk based scaffold developed in house has the novelty for tissue engineering fibro-cartilaginous enthesis i.e. the bridge between bone and ligament. Such a complex graft with incorporation of enthesis in laboratory can provide natural insertional strength at the interface and can change the current scenario of replacing injured ligaments.

KEYWORDS: *Enthesis, Anterior Cruciate Ligament, Interface Tissue Engineering, Knitted Silk, Hydroxyapatite, Chitosan, Gelatin*

CHAPTER -1
INTRODUCTION

1 INTRODUCTION

1.1 INTRODUCTION TO LIGAMENT

Ligaments are comprised of a cellular component and extracellular matrix component[1]. Ligaments contain a variety of cell types, including fibroblasts, fibro cartilage cells and, occasional, fat cells. Fibroblasts are the most common and can be found in all regions of ligaments. They are typically arranged in elongate rows within the parallel bundles of collagen fibers with rod or spindle-shaped fibroblasts (Lin et al. 2004).

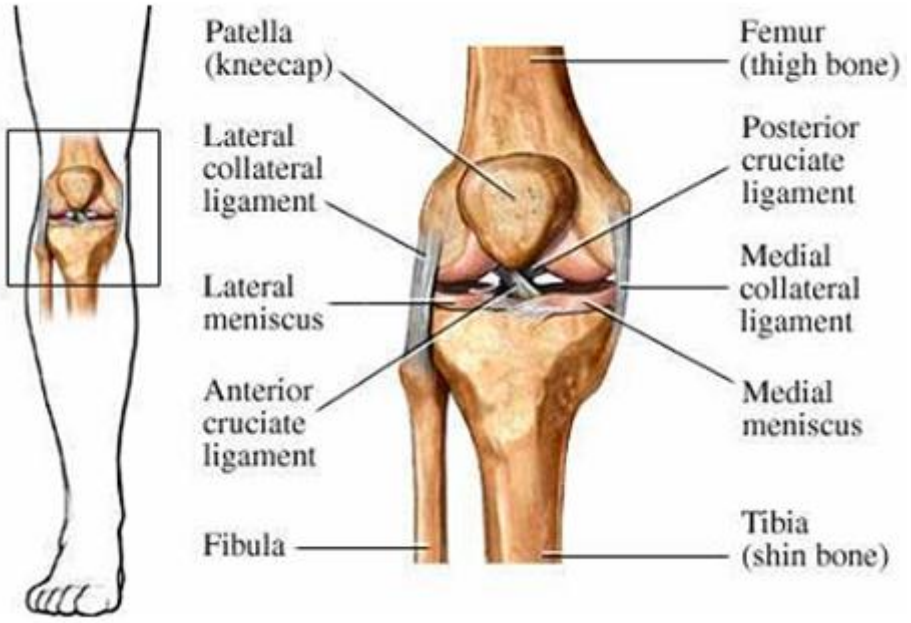

Figure 1: Ligaments of Knee Joints [2]

However, while the fibroblasts do not occupy a large volume of ligament tissues; the cells are responsible for secreting and maintaining the ECM component within the tissue. Relatively low cell population along with their low mitotic activity, may be the reason why ligaments seem to possess a poor healing capacity (Louie et al. 1998). Ligaments have more cells, a higher DNA content and greater amount of reducible crosslink between collagen fibers. Water contributes 60% or more of the wet weight of ligaments. A significant part of this

water is associated with the ground substance which refers to the portion of the matrix consisting of proteoglycans. This part of water plays crucial role in providing lubrication and spacing to the gliding function at the intercept point where fibers cross in the tissue matrices[3]. Four classes of matrix macromolecules (collagens, proteoglycans, elastin, and glycoproteins) contribute approximately 40% of the wet weight of ligaments. Ligaments contain predominantly type I and III collagens. Type I collagen comprises approximately 90% of the collagen in ligaments whereas type III collagen accounts for approximately 10%. Similarly, there is a bimodal distribution of collagen fibril diameters in ligaments, the majority of which are 40 to 75 nm in diameter, with a small number of fibrils are between 100 and 150 nm in diameter (Amiel et al. 1984; Amiel et al. 1990; Goh et al. 2003). Elastin only comprises less than 5% of the wet weight of ligaments. When exposed to mechanical loading, elastin will change from a random coiled structure to a more ordered configuration. This organization change contributes a small part of the tensile resistance in ligament and helps restore the crimp pattern of the collagen fibrils after deformation (Buckwalter et al. 1987).

Ligaments contain two classes of proteoglycans: articular cartilage type proteoglycans and smaller proteoglycans that contain dermatan sulfate. The articular cartilage type proteoglycans maintain water in the tissue and alter fluid flow during loading. Small dermatan sulfate proteoglycans (mainly decorin and biglycan) usually lie on the surface of collagen fibrils and affect the formation, organization of the collagen fibrils (Buckwalter et al. 1987).

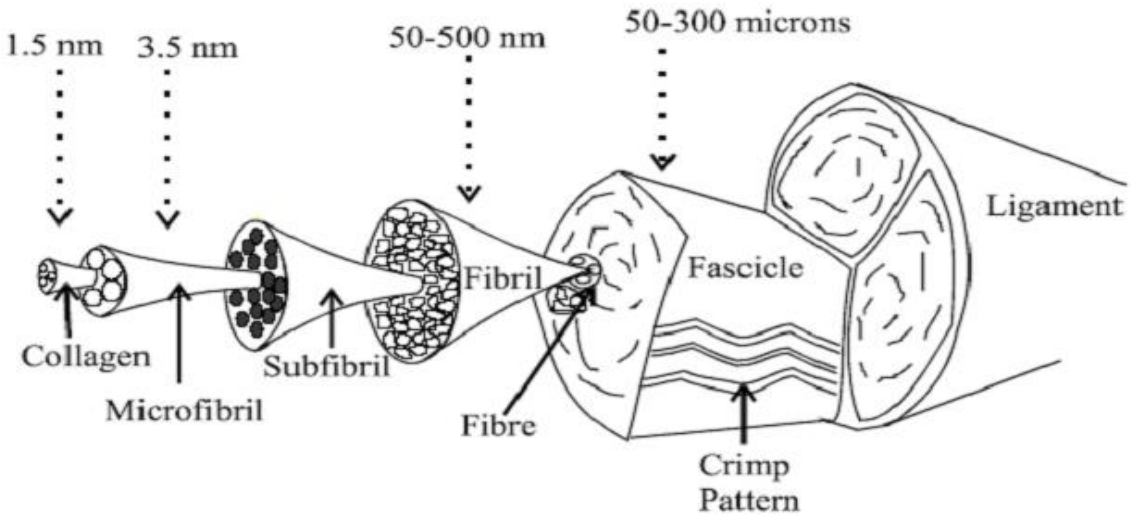

Figure 2: Schematic diagram of the structural hierarchy of ligament [4, 5]

1.2 INTRODUCTION TO BONE

The bone is the strongest and one of the hardest tissues in the body. Due to its composition of calcium and phosphate minerals interlinked to form a hard hydroxyapatite compound, the strength of the bone is known to be phenomenal, along with the enamel minerals found in the teeth. This connective tissue forms the basic skeleton of the body, giving it shape and support to other organs to hold them in place and to facilitate the function of motion and movement. The histology of the bone consists of the basically three kinds of cells – the regular representative cells of the bone known as Osteocytes, the stem cell component of the tissue known as osteoblasts, and the macrophage-like cells of the bone which are responsible for the decay and disposal of dead bone cells and minerals, known as Osteoclasts . The cells are surrounded by a mineral extracellular matrix mostly consisting of calcium-phosphate phase crystals known as hydroxyapatite[5]. The connection and the communication of cells within the tissue and with that of the ones outside are carried out by micro-channels, usually known as Harvesian canals, which carry the nutritional components towards the various cells of the bone. There

are other micro-channels which interconnect the cells to one another within the mineral matrix; the principles of the flow of materials through these channels and the study of their effect on the cells are all investigated as part of micro fluidics branch of research. The bones are connected to each other via ligaments and to that of the muscle via tendons. The joints between two bones where movement is involved are usually articulate in nature with the arrangement of ball-and-socket architecture which facilitates the movement of two bones onto each other. The ligament usually integrates deep within the bone, embedded at the point of contact between the two tissues[6].

1.3 INTRODUCTION TO ENTHESIS

Enthesis is defined as that region of the body which forms a junction between a bone and a ligament. This is one of the least known tissues of the body; however it is one of the most important regions when it comes to ligament tissue engineering and clinical ligament tissue graft replacement. It is a small cartilaginous portion which is present at the junction where a bone and a ligament meet up. It is mainly composed of collagen type 1 and chondrocytes. Depending on the position of the enthesis in the body[7], it can be classified to be of the following types:

(i) Fibrocarilatilaginous: this type of enthesis is the most common type and is the most crucial type of tissue present at the anterior cruciate ligament. This type of enthesis is formed when the junction between a bone and a ligament[8] is occupied by fibrous cells and they secrete their extracellular matrix in the surrounding region. Their thickness is varying depending on the site of their presence.

(ii) Tendonous: this is the thickest type of enthesis present in the body. It is formed when the initial enthesis of the fibrocartilage origin matures and forms the tendon [9]of the body. They are found mostly in the tendon region which connects a bone to a muscle.

(iii) Calcified: at few regions, the enthesis tends to be calcified, especially when present at close proximity to the bone[10]. They form a transition between the ligament/tendon towards the bone and form a continuum between the two different tissue.

Sometimes, it so happens that due to infection or complications of surgeries, the enthesis tends to develop lesions or get inflamed leading to its disintegration. These diseases which affect the enthesis are known as enthesopathies. During these times the joint between a bone and ligament weakens and can lead to rupture or breakage of the bond leading to fractures or other injuries. Hence it is important that these damaged enthesis be replaced by a possible tissue engineering methodology. These methodologies are also made use of during ligament damage and ligament replacement experiments. Fibro cartilage types of enthesis is one of the most common types of enthesis in the body and hence are most preferred type of enthesis for tissue engineering experiments.

1.3.1 Anatomy of Enthesis

The osteotendinous/osteoligamentous junction or enthesis is designed to allow smooth transmission of force between tendon or ligament and bone. An enthesis can be either fibrous or fibro cartilaginous, formed by intramembranous or endochondral ossification, respectively. Indirect fibrous insertions are characterized by soft tissue attachment to the periosteum(a membrane that covers the outer surface of all bones, except at the joints of long_bones), and the presence of Sharpey's fibers that extend directly from the tendon/ligament to the bone. Fibrocartilaginous enthesis are more complex.

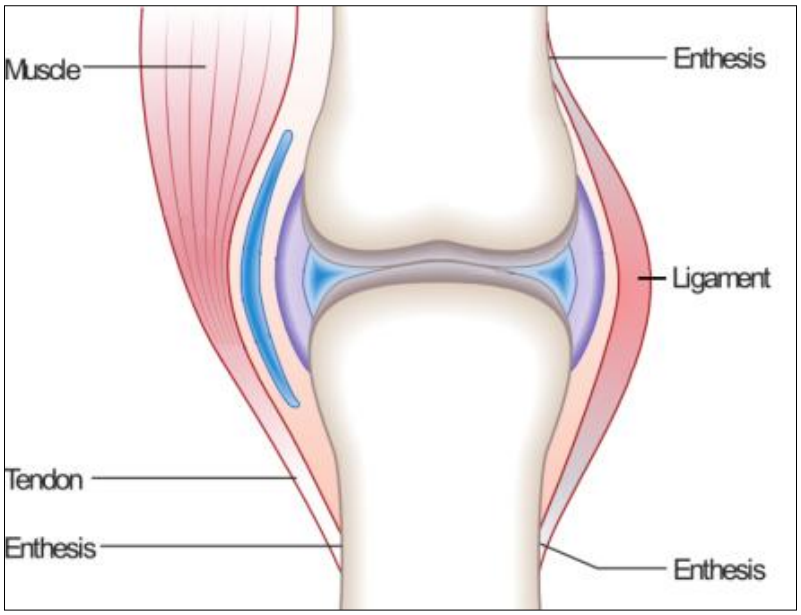

Figure 3: Anatomy of Enthesis [11]

1.3.2 Injury at the enthesis

The most common injuries occurring at the enthesis are sporting injuries, such as the overuse injuries, tennis/golfer's elbow and jumper's knee[12] . Tennis elbow occurs at the junction of the flexor tendons to the humerus and is characterized by the formation of a disorganized collagen matrix at the interface whereas Jumper's knee affects the interface of the patellar tendon with the lower portion of the patella . In addition to overuse injuries at the enthesis, other disorders at the enthesis can also occur. Enthesesopathies are considered insertional disorders and inflammatory disorders are termed enthesis . Entheseopathies can occur in conditions such as diffuse idiopathic skeletal hyperostosis (DISH), a degenerative condition whereby excess bone in deposited at the insertion site . Enthesis is commonly present in the enthesis region of patients with inflammatory disorders such as seronegative spondyleoarthropathies[13].

1.4 TISSUE ENGINEERING FOR ACL REGENERATION

During the damage of a ligament, it is mostly seen that the tissue samples are obtained from an exterior source, which is either an autologous source (the patient's own body) or from a cadaver or another species altogether. However many a times these surgeries and replacements of ligaments fail because the ligament which is fixed into a bone by drilling it within the bone cavity fails to form a reintegration joint with the bone. This leads to loosening of the bond between the two and ultimately failure of the graft.

Scientists all over the world were perplexed as to the reason why a successful graft transfer surgery would fail within months, and the ligament would fail to establish to form a contact with the bone. It was after several close studies that a group of scientists discovered that though the ligament forms the connection between two bones, there was another tissue which formed the connection between a ligament and a bone too. This tissue which was later found to be fibro cartilaginous in nature was established as the enthesis tissue present in various ligament and tendons joints of the body.

It was then that the scientists who were working on the preparation of a tissue graft and other tissue engineering experiments were made aware that preparation of just the ligament would not suffice, and that it was necessary that the enthesis tissue be engineered also along with the tendon so as to form an easy bonding between the bone and the ligament and help speed up the reintegration process. For this purpose, various experiments were then carried out for the tissue engineering of the enthesis tissue. The various steps that were included in it were the fabrication of a suitable matrix to hold the cells, seeding of cells and growing them in a bioreactor providing suitable growth conditions for the ACL and other ligaments.

1.5 OBJECTIVES OF STUDY

In the light of the recent developments in ligament tissue engineering, numerous attempts have been carried out to fabricate the perfect scaffold for the growth and grafting of ligament cells. The current study proposes to fabricate a complex multi -compartmentalized scaffold which will support the growth of three different cell lineages (mature bone cells, ligament fibroblast and stem cells that can differentiate into cartilage) so as to tissue engineer a bone-ligament-bone graft in vitro.. Thus, the objective of the study is the Fabrication of a knitted silk-based scaffold comprising of coatings of different biopolymers for different compartments which can support the mature cell lines (osteocytes, ligament Fibroblasts) and/or induce the stem cells into cartilage cells. The objectives of the current Project is elaborated below:

1. To fabricate a knitted-silk based multi-compartment scaffold reinforced with customized biopolymers i.e.
    a. HA in bone compartment using alternate soaking technology
    b. Gelatin coating for fibrocartilage (enthesis) compartment
    c. Silk-chitosan coating for ligament compartment
2. To characterize and compare the morphology, structural integrity and mechanical strength of each compartment with that of raw knitted silk.
3. To validate the biocompatibility of each compartment through cell attachment and cell-proliferation assays.
4. To validate the morphological and biocompatibility features of the proposed multi-compartmental scaffold after assembling the compartments by suturing.

CHAPTER -2

LITERATURE REVIEW

2 LITERATURE REVIEW

2.1 INTRODUCTION TO LIGAMENT TISSUE ENGINEERING

The anterior cruciate ligament is a collection of regularly oriented, dense connective tissue which connects the femur to the tibia. The Anterior cruciate ligament inserts into bone through an interface region called (enthesis) and serves as a joint stabilizer by acting as the primary restraint to anterior tibia translation. Tear of ACL are the most common Knee ligament injuries which affect over 100,000 people per year in the U.S. Most of the ligaments injuries occurs at the ligament to bone insertion, particularly at the femoral insertion site.ACl exhibits poor healing potential with its limited vascularisation, ruptures ACL don not heal for this surgical intervention is required. There are two currently options are required which helps to reconstructs the ruptures ACL, which are autologous based reconstructions are: bone-patella-tendon-bone (BPB), and hamstring tendon based grafts. There are limitation associated with BPB grafts , so Use of hamstring tendon based grafts has increases e.g. donor side morbidity ,muscle atrophy ,tendonitis and arthritis. The maximum clinic usage of the hamstring tendon based grafts is hindered by its inability to fully integrate with bone and the associated increase in knee laxity due to inadequate graft fixation.

The native anterior cruciate ligament to bone insertion mainly consists of four different tissue regions are: Ligament, non-mineralized interface, mineralized interface and bone.

- The ligament region is mainly composed of fibroblast embedded in type I and type III collagen matrix.
- The non-mineralized interface regions mainly consist of ovoid chondrocytes and type II collagen is present within pericellualr matrix and the primary sulphated proteoglycan is aggrecan.

- The mineralized interface region consist hypertrophic chondrocytes that are surrounded by extensive pericellular matrix. Type X collagen is associated with hypertrophic chondrocytes which is mainly found only within the mineralized region. At last the overall interface region looks like a fibro cartilaginous tissue.
- The last region along the ligament insertion axis is the subchondral bone, in which osteoblasts, osteocytes and osteoclasts are embedded in,a type I collagen matrix.

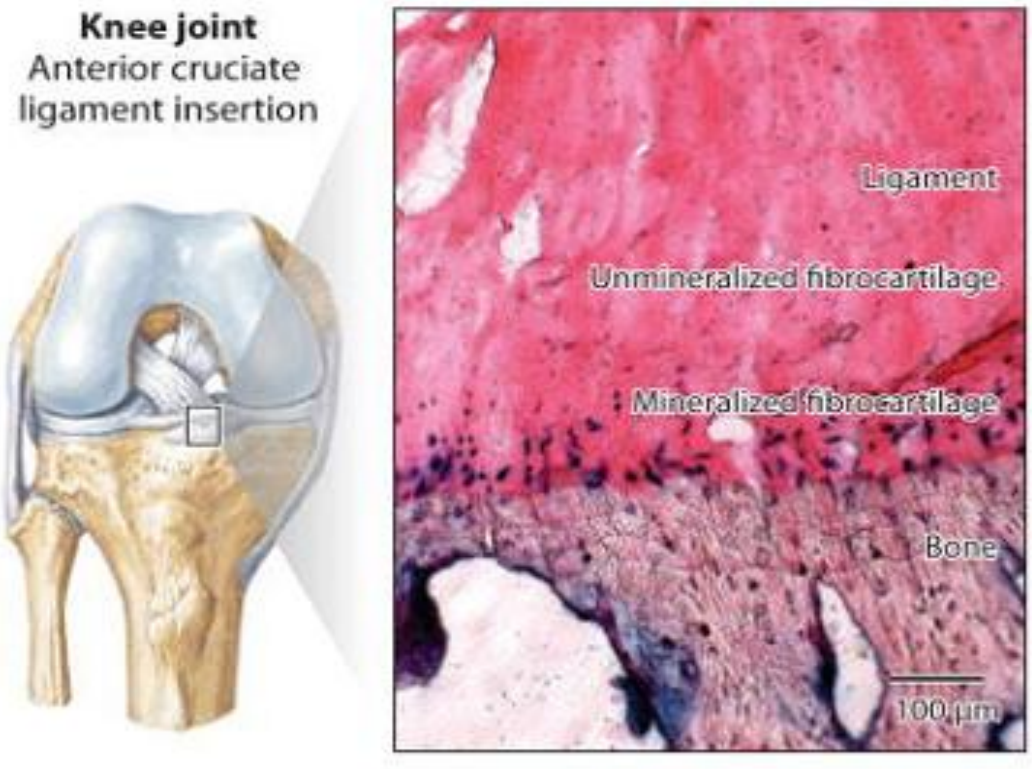

Figure 4: Four different tissue regions of ligament to bone insertions[14]

The ideal scaffold for interface tissue engineering [15] strongly support multi-tissue regeneration, which stimulate homotopic and heterotypic cell interactions, and facilitates the development of different cellular and matrix zones mimicking those of the local insertion. In

addition to supporting cell attachment and growth, each phase of the scaffold should be designed to ensure that controlled morphologic and chemical stimuli are present to promote phase and tissue-specific matrix amplification. Other tissue engineering applications, the interface scaffold must be biodegradable in nature and exhibit mechanical properties comparable to those of the native ligament-to-bone insertion site.

2.2 INTERFACE TISSUE ENGINEERING

Various Tissue engineering experiments were commenced for the fabrication of a suitable ligament tissue graft to overcome the aforementioned problems. Novel 3-dimensional scaffolds were synthesized using various natural and synthetic products in order to provide the mechanical support and strength for growth of ligament cells. It was later observed that the ligaments grew well in-vitro and the formation of the tissue in laboratory conditions were perfect; nevertheless when the scaffold was transferred into the body to help the synthesized ligament implant within the knee, inserts itself within the tibia and femur, it was found that the tissue graft failed to integrate within the bones of the knee. Various reasons were brought into light for the failure of the experiments – early biodegradation of the scaffold, loosely fixation of the scaffold at the site of injury, toxicity caused by the material of the scaffold etc.

The most important reasons for the tissue graft failure was found to be the failure of the ligament to reintegrate with the bones of the femur and tibia at the cellular and molecular level. Studies revealed the presence of a specialized tissue which was comprised of fibro cartilaginous cells at the junction where the bone and the ligament meet called Enthesis[16]. Scientists perceived that the failure of the tissue graft lied in the structural component of the artificial ligament where the enthesis was not present as a part of

the organ. This proceeds to further advancements in scaffold engineering experiments where the enthesis was included as an integral part of the scaffold along with the ligament and bone.

2.3 APPROACHES OF INTERFACE TISSUE ENGINEERING

Interfacial tissue engineering approaches aim to replicate the micro- and nano-structure of the interface in the form of advanced scaffolds, or replicate the complex cellularity or biochemical composition of the interface through cell co-cultures and growth factor gradients. These strategies are focused either to generate the interface alone, or to generate it as part of an integrated multi-organ complex, such as a bone-ligament graft or an osteochondral plug.

The approaches can be roughly grouped into the following categories:

- Scaffold-based strategies: multi-phased scaffolds;
- Cell-based strategies: stem cells and co-cultured cells;
- Growth factors and gene therapy;
- Mechanical loading in bioreactors.

2.4 BIOMATERIALS USED FOR REPAIR LIGAMENT INJURY

ITE focuses on the development of engineered tissue grafts capable of replacing normal function in the defective interfaces[17]. Tissue interfaces, such as ligament-to-bone, tendon-to-bone and cartilage-to-bone, exhibit anisotropic structural properties, which gradually vary from one tissue to another. Soft tissue reconstruction methods using conventional isotropic scaffolds do not result in adequate synthetic graft integration to bones. The lack of integrating interface greatly affects the graft function. This is mainly due to the use of homogeneous biomaterials (either compositionally or structurally) to engineer tissue grafts that do not support the growth of heterogeneous cell populations that reside at the interface tissues. As a

result, the implants do not fulfil their intended function, which ultimately leads to graft failures. To engineer interface tissues, a bio mimetic scaffold with graded properties is therefore useful, especially since physical and chemical cues provided by the scaffold materials effect the fate of cultured cells. In a notable example, Engler et al. Showed that mesenchymal stem cells could differentiate into different lineages, such as neurons, myoblasts and osteoblasts, depending on the cell culture substrate's stiffness such a gradient scaffold should provide an optimal environment to direct both heterotypic and homotypic cell–cell communications, as well as cell–matrix integrations. It should also support cellular growth and differentiation to form a graded tissue at the interface. In summary, the scaffold used to generate an interface tissue should exhibit a gradient in composition, structure and mechanical features, among other functional properties, mimicking those of the native interface zones. The advancement of micro- and nanotechnologies enable us to develop tissue scaffolds with gradient in material composition and properties that enable spatially controlled differentiation of cells and subsequent tissue development.

The multi-tissue transition from ligament to bone at the ACL -to -bone interface represents a significant challenge for functional interface tissue engineering. Inspired by the native interface, Spalazzi et al. pioneered the design of a tri- phasic scaffold for the regeneration of the ACL to bone interface. The scaffold consists of three continuous phases, each engineered for a specific tissue region of the interface: Phase A is a polymer fiber mesh for fibroblast culture and soft tissue formation, Phase B consists of polymer microspheres and is the interface region designed for fibro chondrocyte culture, and Phase C is comprised of sintered polymer- ceramic composite microspheres for bone formation [18] (Lu et al. 2003).

2.5 SCAFFOLDS FOR INTERFACE TISSUE ENGINEERING

The scaffold is innovative in that it is in essence, a "single" scaffold system with three distinct yet continuous phases, designed to support the formation of the multi -tissue regions observed across the ligament-bone junction. To form the ligament, interface and bone regions, fibroblasts, chondrocytes and osteoblasts were seeded onto Phases A, B and C, respectively. Interactions between these cell types on the stratified scaffold have been evaluated in vitro and in vivo[19]. Extensive tissue infiltration and abundant matrix deposition with tissue continuity maintained established across scaffold phases. Interestingly, matrix production compensated for the decrease in mechanical properties accompanying scaffold degradation, and three continuous regions of ligament, interface and bone-like matrix was formed in vivo[19] .

CHAPTER-3
PLAN OF WORK

3 WORK PLAN

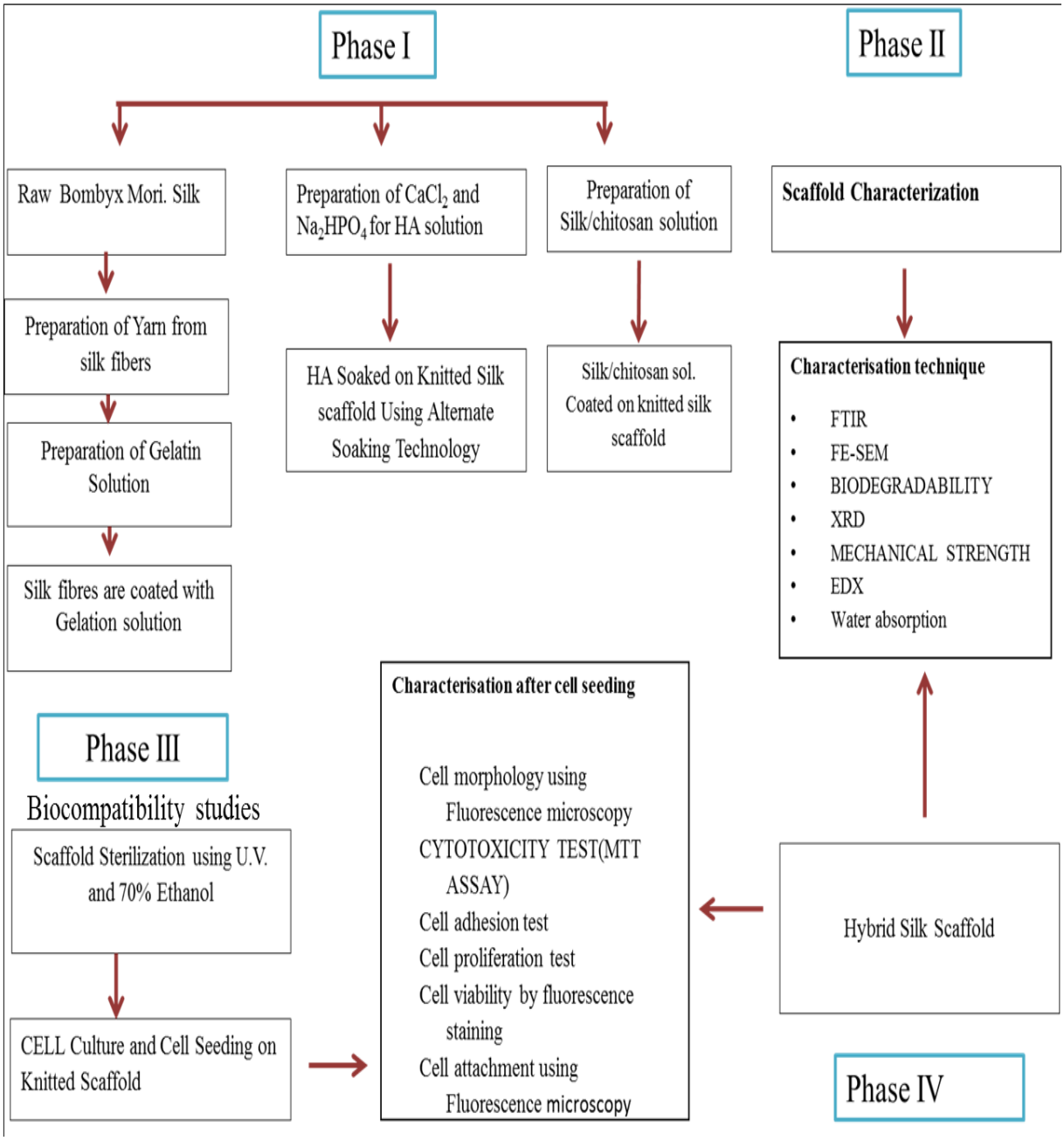
Phase I
Phase II
Raw Bombyx Mori. Silk
Preparation of Yarn from silk fibers
Preparation of Gelatin Solution
Silk fibres are coated with Gelation solution
Preparation of $CaCl_2$ and Na_2HPO_4 for HA solution
HA Soaked on Knitted Silk scaffold Using Alternate Soaking Technology
Preparation of Silk/chitosan solution
Silk/chitosan sol. Coated on knitted silk scaffold
Scaffold Characterization
Characterisation technique
FTIR
FE-SEM
BIODEGRADABILITY
XRD
MECHANICAL STRENGTH
EDX
Water absorption
Phase III
Biocompatibility studies
Scaffold Sterilization using U.V. and 70% Ethanol
CELL Culture and Cell Seeding on Knitted Scaffold
Characterisation after cell seeding
Cell morphology using Fluorescence microscopy
CYTOTOXICITY TEST(MTT ASSAY)
Cell adhesion test
Cell proliferation test
Cell viability by fluorescence staining
Cell attachment using Fluorescence microscopy
Hybrid Silk Scaffold
Phase IV

CHAPTER - 4

MATERIALS AND METHODS

4 MATERIALS AND METHODS

4.1 FABRICATION OF SCAFFOLD

4.1.1 Preparation of Silk Yarn

Silk fibres were procured from (Raw tassar Silk Depot, Chiabasa, and Jharkhand, India). Out of the many types of silk fibers that were procured, the silk strand having 12 fibers was made use of. The fibroin was stretched and woven around to form a 12-threaded yarn which was then braided to result in a cluster thread of roughly 2mm thickness. This silk thread was used further to prepare the knitted-silk base for the scaffold[20].

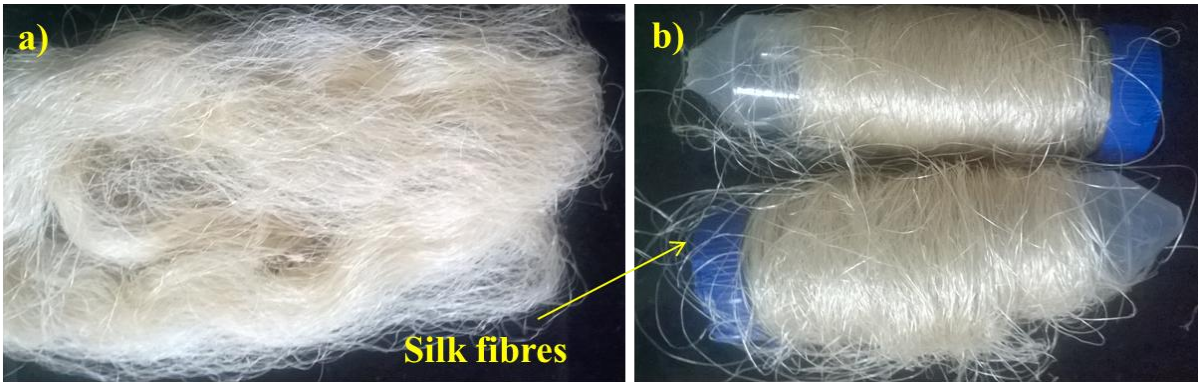

Figure 5: a) Raw B.mori Silk fibres b) Prepared Silk Yarn

4.1.2 Preparation of Gelatin Solution

Gelatin Crystals From Himedia(CAS No:9000-70-8) were mixed with distilled water (H_2O) and then gently stirred at 40^{o}C For 1 hour to obtain 50 ml of 6 wt% of Gelatin solution[21].

4.1.3 Knitting of Gelatin coated Silk fibers

The Gelatin coated silk f threads were used to make yarns which were knitted **using Brother Knitting Machine** (Model no. KH830) using 6 alternative needles to obtain a patterned mesh of dimension 2cmX6cm with preset pore patterns. To carry out the knitting, six alternate

needles were pushed to ‘Out’ position. The yarn threads were loaded to K-carriage and pulled towards the right end. The six needles were shifted to Working’ position. The ‘Claw’ weights were used to provide uniform force towards the ground during knitting process to direct the knitted silk downwards. The K-carriage was alternatively slid left and right over the six needles to commence the knitting process. Once knitting was completed, the remaining yarn was cut about 10cm from the main knitted silk and the K-carriage was moved away from the knitted silk.

The knitted mesh was then tied on to a rectangular glass slide of dimension 3cmX8cm such that the mesh is exposed on one side of the glass slide which can be used for coating of polymers and cell seeding during later experiments; and extensions of the thread flanking from either sides of the mesh were used to tie a knot behind the glass slide to keep the silk mesh intact in its position. This constituted of the knitted-silk base which was used for all subsequent experiments[22].

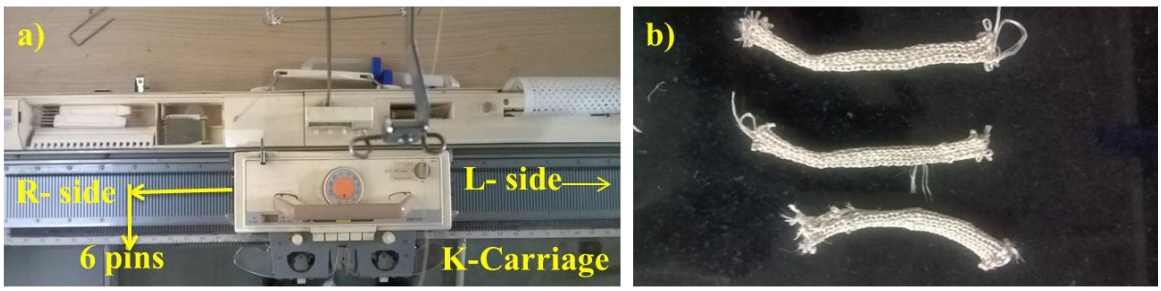

Figure 6: a) Knitting Machine b) Knitted Silk fibres

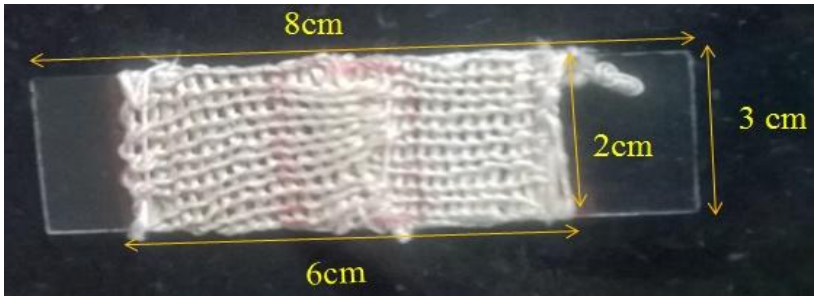

Figure 7: Knitted Silk Scaffold Tied on 3 cm X 8 cm Glass Slide

4.1.4 Morphological characterization of gelatin coated knitted silk

4.1.4.1 FE-SEM Analysis of Knitted Silk Scaffold

The morphological characterization of the knitted silk base was carried out in (FEI-NovaSEM 450) field emission scanning electron microscope using gold coating. The knitted silk was cut into small square pieces of dimensions suitable to load on the sample holder of the device. The fibres were subjected to sputter coating of gold for 5 minutes prior to visualization of the same under the microscope. The knitted silk was observed under an electric field of 20KV and was visualized at 30x magnification.[23]

4.1.4.2 Preparation of Phosphate Buffered Saline

Phosphate Buffered Saline (PBS) is one of the most important buffers used in vitro studies and for preparation of experimental solutions, due to its constituent and parametric resemblance to the body fluids. 1L of 1X PBS solution was prepared. Then 8g of NaCl was mixed thoroughly followed by 0.2g of KCl. This was followed by the addition of 1.44g of Na_2HPO_4 and then KH_2PO_4. The pH of the solution was adjusted using 1N NaOH and 1N HCl until the value was set at 7 at 25ºC.[24]

4.1.5 Mechanical Strength Testing

The study of mechanical tensile strength of a scaffold is one of the key parameters in the design of an ideal scaffold. The objective of the study is to make sure that the scaffold is strong enough to bear mechanical load in regions that it is implanted. Additionally it also gives an idea of the degradation rate of the scaffold when present in an environment of body fluids.

The knitted-silk meshes were immersed in Freshly prepared 1X Phosphate Buffer Saline (PBS) adjusted to pH-7 at 37ºC for a duration of 3, 7, 14, 21 and 31 days. The pH of the buffer was adjusted using 1N HCl and 1N NaOH solutions as per requirements. Once the stipulated time was completed for each knitted-silk mesh, it was taken out of the buffer solution, dried and tested for mechanical tensile strength using (TA-HD Plus Texture Analyser) where the gauge length was set at 20mm and cross head speed was maintained at 10 mm/min uniformly for all the meshes[25].

4.2 POLYMER COATING ON KNITTED-SILK SCAFFOLD

4.2.1 Preparation of Silk Solution

Silk solution was prepared using raw silk cocoons of *Bombyx mori* silkworm. The cocoons were first cut into two halves and the carcass of the worm along with any dirt or impurity was removed. The cocoons were then cut into very fine pieces boiled in degumming solution for 3 hours with regular change of the solution every half an hour. The degumming solution, which is made of 2% (w/v) Na_2CO_3 dissolved in distilled water, is basically used to remove the antigenic serecin from the silk fibroin so as to prevent immunogenic response once the final scaffold is implanted into the body. Once the cocoons are boiled in the degumming solution, they are removed and washed in running distilled water close to 20 minutes and air dried

overnight. The dry degummed silk fibres are then dissolved in 98% formic acid solution at room temperature at different concentrations (w/v) as per requirement of the experiment. The silk fibres were stirred overnight at room temperature for complete dissolution in the solvent[26].

4.2.2 Alternate Soaking Process - Hydroxyapatite Synthesis

For Hydroxyapatite synthesis initially we prepared 120mM solution of Na_2PHO_4 in 0.1M Tris base solution. This solution was called Solution-(A). Secondly 200mM solution of $CaCl_2$ was prepared in the same buffer and called Solution-(B). The partially covered knitted scaffolds were first immersed completely in solution A for 30 minutes, then removed from the solution and was blotted for excess solution before immersing it in solution B for the same duration. Likewise they were alternately immersed completely in both these solution for a total of 10 cycles. The scaffolds after 1, 2, 3 and 4 cycles of alternate soaking were respectively chosen as principal samples for further studies. The samples were then subjected to serial dehydration by immersing them in ethanol solutions of increasing concentration – 30%, 50% 70% and 100% (all percentages are in v/v ratio)[27, 28]. These scaffolds were then sealed in airtight containers and stored until they were used for further analysis and other experiments.

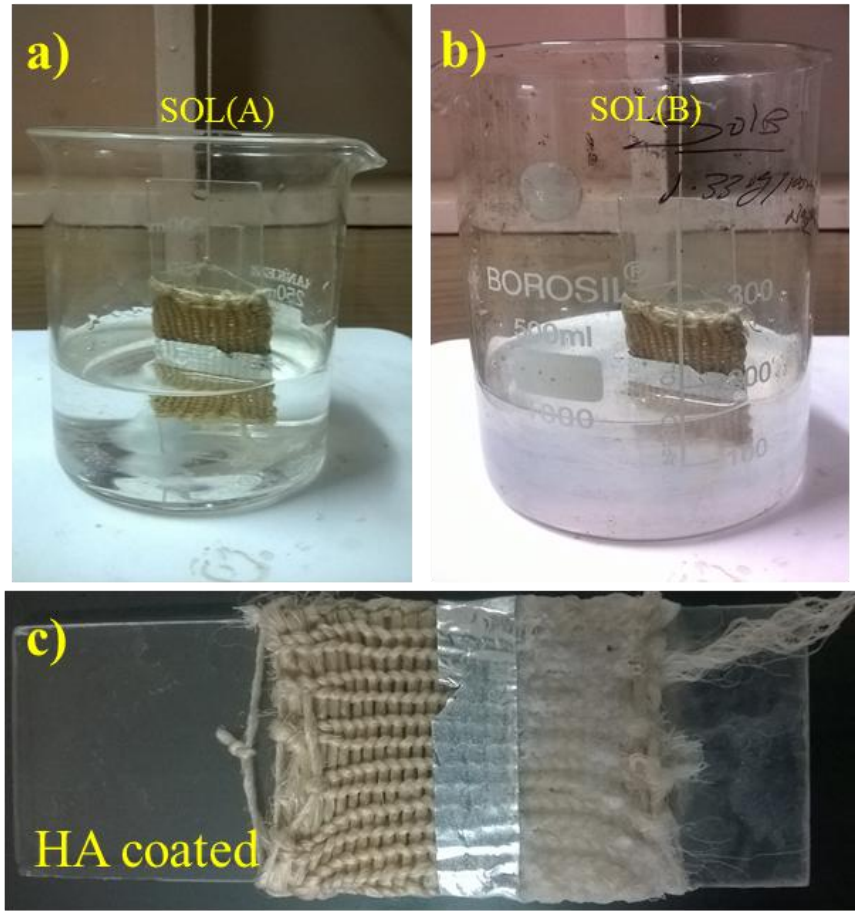

Figure 8: a) Sol A $CaCl_2$ b) Sol B Na_2HPO_4 c) HA Soaked knitted scaffold

4.2.3 Freeze Drying Process or Lyophilisation – Silk/Chitosan solution

Silk/chitosan blend solutions were prepared by dissolving equal amounts of silk and chitosan in 98% (v/v) formic acid and 2% (v/v) acetic acid respectively. Both silk and chitosan were added in increasing amounts – 2%, 4%, 6%, 8% (w/v) - in their respective solvents stirred at 60ºC until all the particulates have dissolved in the solvent. The solutions of the two polymers were mixed together such that the resultant solution contained equal concentration of both silk and chitosan. Knitted-silk fibers were immersed into the these solutions and subject to lyophilization using (operon chemical free freeze dryer, Korea) to remove the solvent molecules resulting in the coating of silk-chitosan blend over knitted silk base[29].

4.3 CHARACTERIZATION STUDIES OF MODIFIED KNITTED SCAFFOLD

4.3.1 Water Absorption Studies

Water absorption properties were studied for each type of scaffold. PBS solution was prepared at pH 7. Initial dry weights of all three scaffolds noted and then they were immersed in PBS at 37ºC (denoted as W_0). The weights of scaffolds were monitored every 60 minutes and were immersed back in fresh PBS solution under the same conditions. The newly acquired weights were noted until there was no recurrent change in the weight of the sample (final weight denoted as W_n where 'n' the last immersion step). This was assumed to be the maximum absorption capacity of the scaffold. The water absorption percentage of the scaffold was calculated using the following formula:

$$\% \text{ Absorption} = \frac{\text{Wn} - \text{W0}}{\text{W0}} \text{ X } 100$$

The absorption capacity of water depends upon the affinity of the scaffold material over with water molecules and the size of the scaffold. Keeping this in mind, the absorption study was

carried out keeping all the sizes of each category of scaffold same among themselves. Hydroxyapatite coated scaffolds were studied using a uniform size of 60mm X 20mm dimensions. Silk/Chitosan scaffolds were kept at a uniform dimension of 30mm X 20mm[22, 30].

4.3.2 Field Emission Scanning Electron Microscopy (FE-SEM)

Topology study of the hydroxyapatite-coated scaffold was carried out using (FEI-NanoNovaSEM 450) field emission scanning electron microscope. The four main sample scaffolds of alternate-soaking experiment were cut in appropriate dimensions and sputter coated under vacuum with particulate gold for duration of 2 minutes. The scaffolds were then shifted to high vacuum chamber of the FE-SEM and were visually observed for their characteristics at magnifications of 100X, 500X, 2000X and 25000X[31].

4.3.3 EDS (Energy dispersive X-ray Spectroscopy)

For the elemental analysis or chemical characterization of a sample an analytical technique is used Energy –Dispersive X-ray Spectroscopy. It relies an interaction of Source of a sample and X-ray Excitation.

Its basic principle is that each element has a unique atomic structure allowing unique set of peaks on its X-ray emission spectrum. The emission of Characteristic X-rays from a Specimen is stimulated by a high energy beam of charged particles such as electrons or Protons, or a beam of X-rays which acts on sample[32].

4.3.4 Fourier Transform Infrared Spectroscopy (FTIR)

Fourier Transform Infrared Spectroscopy was performed for the hydroxyapatite-coated samples. It was carried out using IR Prestige-21 FTIR Spectroscopy, Shimadzu Corp.

(Japan). The samples were cut into very fine pieces, and pressed into pellets and placed on the sample holder. The IR peaks for the scaffold coated with different concentrations of hydroxyapatite were obtained[33].

4.3.5 X-Ray Diffraction (XRD)

X-Ray Diffraction studies were performed for all three kinds of scaffolds – hydroxyapatite coated, silk/chitosan coated with different concentrations of coatings. XRD was carried out using Rigaku Ultima IV X-Ray Diffractometer at an observational range of 10º-60º with a step size of 0.04º and at a rate of 3º/min. An energy of 2kW under 60kV was supplied to A-41-Copper electrodes emitting beams through a window of 10mm width[34].

4.4 CELL CULTURE & BIOCOMPATIBILITY STUDIES

For the study of cell attachment and cell proliferation on the different types of coatings on the silk mesh, two types were of cells were used, both procured from National Centre for Cell Science, Pune. MG-63, an osteoblast-like cell line isolated from human primary osteosarcoma, was used to study the osteoconductivity properties of hydroxyapatite coating on the scaffold. Saos-2, a fibroblastic cell line derived from human primary osteosarcoma, was used to study the attachment and proliferative properties of silk-chitosan coating on the silk scaffold.

4.4.1 Cell Culture

The culturing and incubation protocols followed for both Saos-2 and MG-63 cell lines were identical. The cells were cultured using DMEM-Low Glucose growth media purchased from Himedia and supplemented with 5% (v/v) fetal bovine serum in a T-75 culture flask. The media was replaced every 48 hours. The culture flasks were periodically examined for

proliferation and confluence. Once the cells reached 80% confluence, they were subjected to sub-culture. Subculture was carried out by initially removing the media from the flask, and subsequent washing of the cells with PBS. This was followed by trypsin treatment where trypsin-varsene solution was washed over the cells and incubated at 37ºC for 2 minutes to detach the cells from the surface of T-flask. They were then washed using DMEM containing FBS to inactivate the enzymatic action of trypsin. The cells, which are now suspended in the latter solution, are subjected to centrifugation at 8000rpm for 5 minutes wherein the cells settle to the bottom of the centrifuge vial owing to the centripetal force. The cell pellets are collected and their concentration is calculated using a Neuber's Chamber. The cells are then appropriately distributed into other flasks in 1:4 ratio as recommended by NCCS Pune[35].

4.4.2 Scaffold Sterilization

The scaffolds were placed in 100mm^2 Petri-dishes, placed inside the biosafety-cabinet and subjected to formaldehyde fumigation. Formaldehyde solution (37%) was kept in another Petri-dish and kept inside the biosafety cabinet along with the scaffolds such that the vapours of formaldehyde penetrate the scaffolds and decontaminate them. This was followed by exposure of scaffolds to UV light for 5-10 minutes and washing with PBS thrice to remove traces of formaldehyde from within the scaffold[30]. The scaffolds were then stored in sterilized desiccator until further use.

4.4.3 Cell Seeding

Cell seeding was carried using regular cell-drop method where cells in media at a concentration of 2.8 X 10^6 cells/ml (MG-63) and 2.3 X 10^6 cells/ml (Saos-2) was seeded over the scaffolds. After an interval of 60 minutes, DMEM supplemented with 5% fetal bovine serum was added to the scaffold. MG-63 cells were seeded over hydroxyapatite-coated scaffold while Saos-2 cells were seeded over silk-chitosan coated scaffolds[25].

4.4.4 Cell Adhesion Study

To find out the concentration of cells attached to the surface of the scaffold, 30mm X 20mm pieces of each scaffold sample (including that of different concentrations of coatings) was used. Cell seeding was performed at a concentration of 2.8 X 10^6 cells/ml (MG-63) and 2.3 X 10^6 cells/ml (Saos-2) as mentioned above and incubated in CO_2 incubator. After 24 hours, the scaffolds were removed from the petri-plates and the media was collected in 15 ml tubes. Further, the petri plates were subjected to trypsin treatment and then washed with media supplemented with serum to dislodge any cells attached to the surface of the petri plate and transferred to same tubes. The washed media was subjected to centrifugation at 8000rpm for 5 minutes and cell count of the pellet was carried out. This cell concentration was subtracted from the initial cell seeding concentration to obtain the number of cells attached to the surface of the scaffold[36].

4.4.5 Cell Proliferation and Viability Assay

MTT assay was carried out to study the cell proliferation over the scaffold. Briefly, MTT solution was added to the cell seeded scaffold bearing culture media at 4µl/100µl concentration along with a sample of plain media (control), and incubated at 37ºC for 30 minutes. Next, formazan was solubilized using 3ml acidic isopropanol solution. The solution was pipetted repeatedly and incubated at 37ºC for 30 minutes to ensure complete dissolution of formazan. Optical density (OD) of the resulting solution was checked at 540nm. Serial dilutions of a known cell concentrate were processed by method described above to obtain a standard plot (OD against cell concentrations). Absolute cell number was counted for studying cell proliferation by matching the ODs in the standard plot[37].

CHAPTER-5

RESULTS AND DISCUSSIONS

5 RESULTS AND DISCUSSIONS

5.1 MORPHOLOGY OF FABRICATED SCAFFOLD

5.1.1 Morphology of Knitted Silk Scaffold

The Gelatin Coated knitted silk scaffold[38], which was prepared using 12-yarn silk fibres and knitted, using Brother knitting machine, was observed at 30X under FE-SEM. The image shows uniformly knitted loops of silk fibres coiled around each other to form a mesh of consistent thickness and interconnectivity. The average pore size of each loop of the knit is found to be around 1mm. A cluster of 12 individual fibres of the yarn looped around each other to render a firm gripped thread can be clearly distinguished in the image.

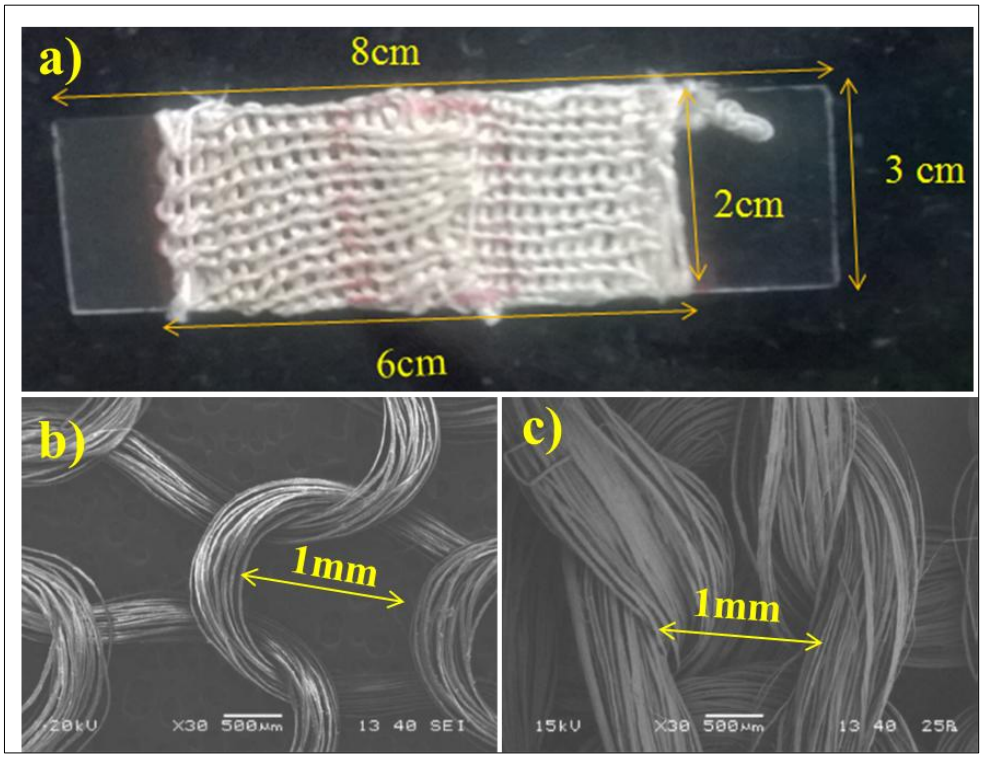

Figure 9: Morphological visualization of a) Knitted silk scaffold b),c)under FE-SEM

5.1.2 Morphology of Hydroxyapatite soaked on knitted silk scaffold

Hydroxyapatite coating over knitted silk scaffold was carried out by soaking the silk fibres alternately in solutions of Na_2HPO_4 and $CaCl_2$. As viewed by the naked eye, it was observed that the scaffold appears to be thicker with the increasing number of cycles of immersion in the two solutions. Handling the scaffolds also revealed that the more the coating of hydroxyapatite over the knitted silk, the less flexible the material became[39].

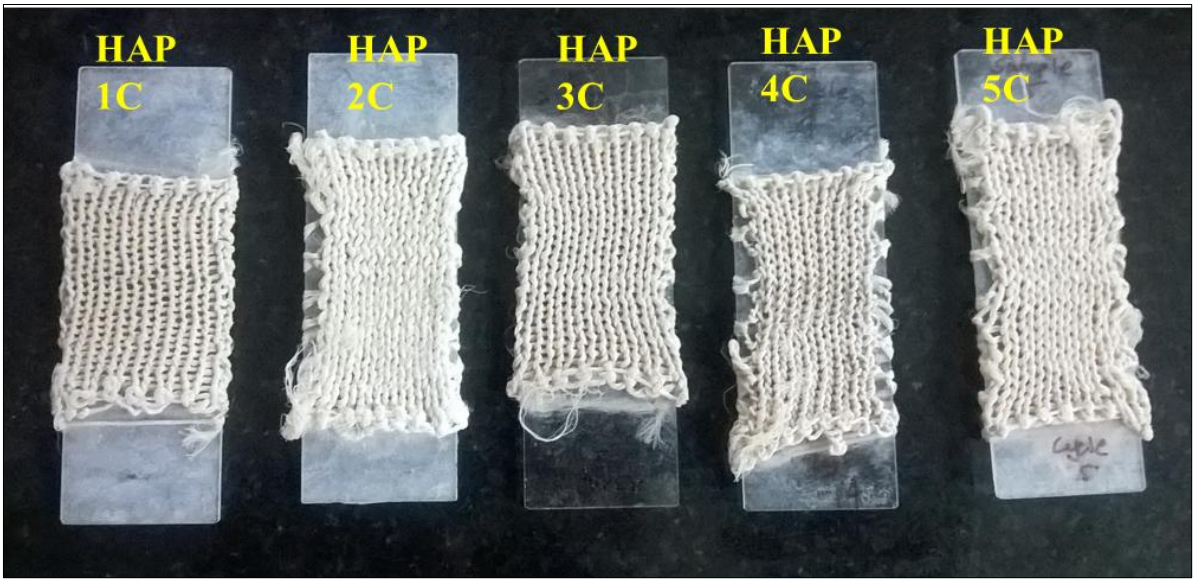

Figure 10: Hydroxyapatite coated knitted silk scaffold using alternate soaking Technology

5.1.2.1 FE-SEM Analysis of Hydroxyapatite Coated knitted silk scaffold

SEM analysis revealed that hydroxyapatite coating was present uniformly throughout the scaffold and all the strands of the fibre. With increasing cycles of soaking, the gap between the fibres of the knitted silk reduced. The thickness of each strand of silk was about 52µm and that of each fibre of the yarn was 585 µm in the first sample of 1cycles of alternate soaking. The corresponding values increased to 131 µm and 921 µm in the 5cycle counterpart of the alternate soaking process.

It was also observed that the morphology of the hydroxyapatite coating over the scaffold was quite unique. As compared to earlier literature which claimed the presence of nano-scale spherical bead-like morphology of the mineral, this study revealed the presence of polygonal flake-like hydroxyapatite coating which were close to 500nm in breadth[40].

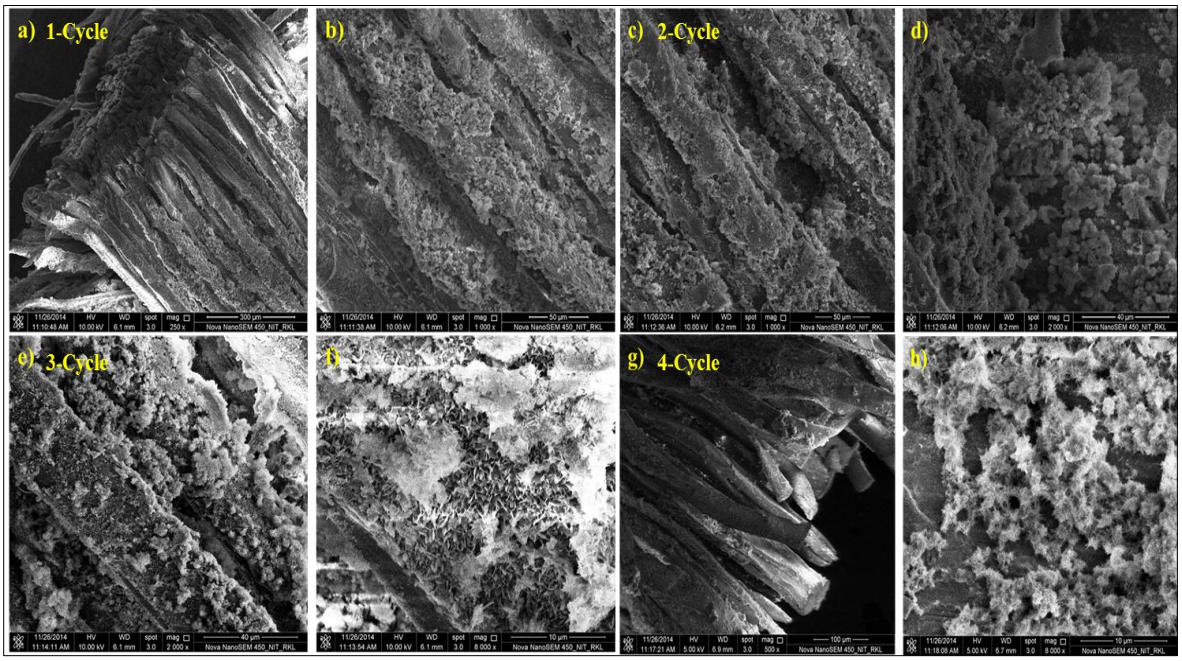

Figure 11: FE-SEM analysis of Hydroxyapatite coated knitted silk scaffold at a),b) 1cycle c),d)2 cycle e),f) 3 cycle g),h) 4 cycle of Soaking

5.1.2.2 5.1.2.2. XRD Analysis of Hydroxyapatite Coating

XRD analysis was carried out to understand the crystallinity of the hydroxyapatite coating formed on the knitted scaffold. Peak intensities around 2θ values of 32º and 26º are indicative of the presence of hydroxyapatite crystals. The sharpness of the peak indicated the fine crystallinity of the hydroxyapatites formed on the knitted silk scaffold[41].

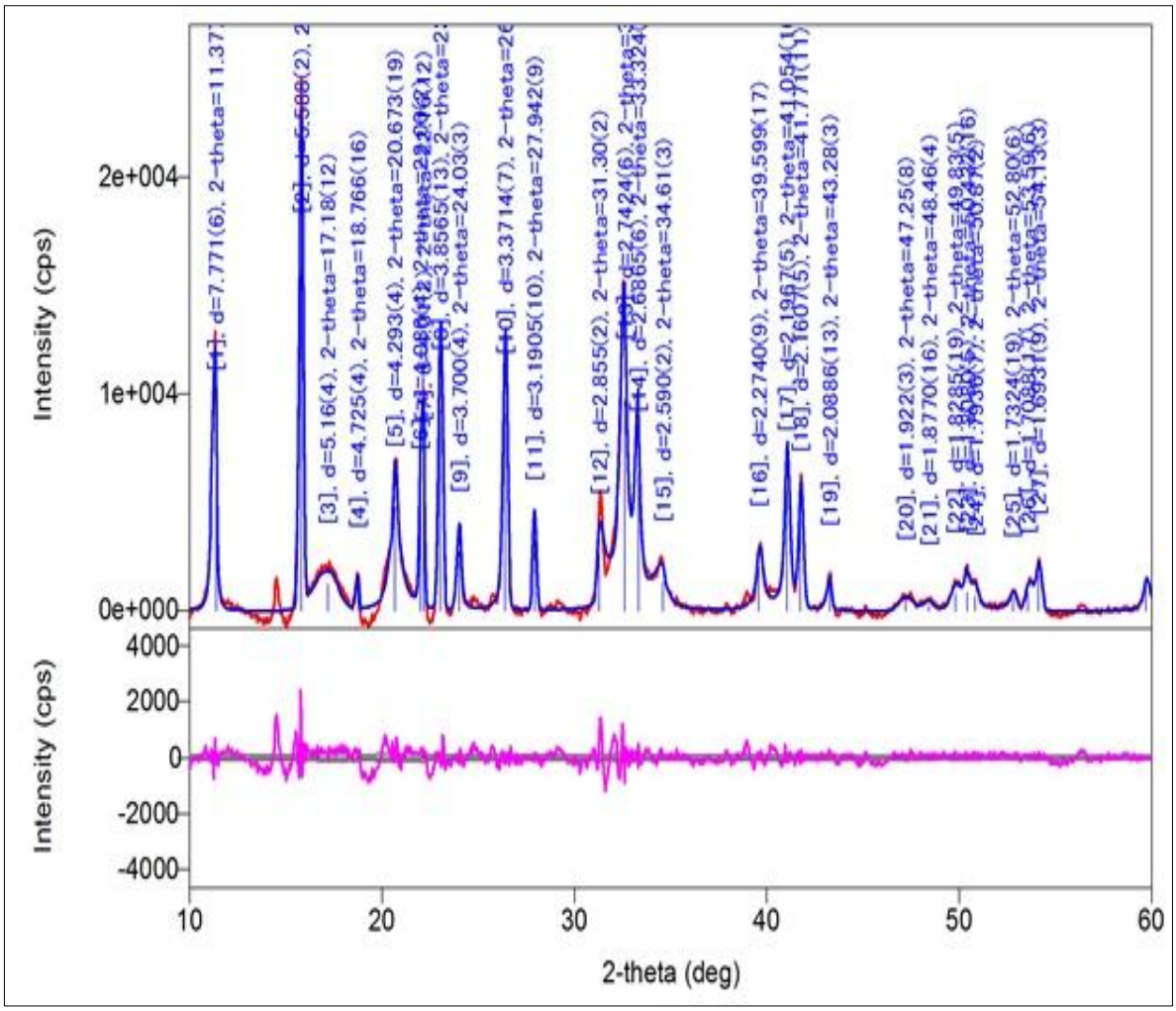

Figure 12: XRD analysis of Hydroxyapatite coated knitted silk scaffold

5.1.2.3 FTIR Analysis of Hydroxyapatite Coated knitted scaffold

FTIR analysis was carried out to determine the bond characteristics and the side chains present in the sample.

Table 1: FTIR Peaks For Phosphate and Carbonate absorption band

Sample Code	Phosphate absorption band(cm-1)	Carbonate Absorption Band(cm-1)
HAP-1	1054	1621
HAP-2	1054	1621
HAP-3	1054	1632

The major peak at around 1250 cm-1 is indicative of the presence of amide III linkage of silk fibroin. For PO_4^{3-} the following bands are assigned 605-419 and 961-1060 cm-1. For H2O observed in FTIR spectra by bands at 2350-2364 cm-1 .The bands around 1515 -1621cm-1 assigned to various C-O stretching vibration modes of CO_3^{2-} ions[42].

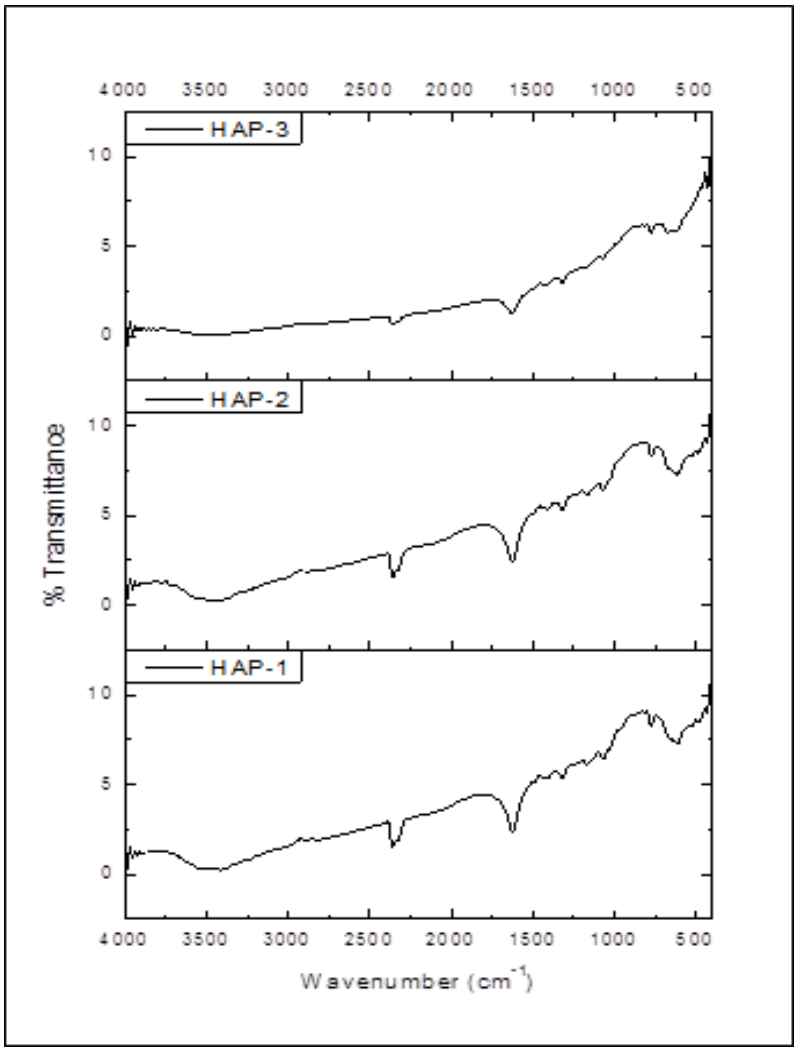

Figure 13: FTIR Analysis of Hydroxyapatite coated knitted silk scaffold

5.1.2.4 EDS studies of Hydroxyapatite coated knitted scaffold

5.1.2.4.1 Elemental analysis of 1 cycle Hap soaked knitted scaffold

In this analysis we analysis the elements present in the Hydroxyapatite (Ca,P,O,H) coated knitted silk scaffold, through this we analyze the hydroxyapatite is present or not by the help of the Ca/p ratio which is less than 2.

Ca/p= 1.67 for Hydroxyapatite

By plotting graph between cps and eV we get the peaks of elements present in that sample like Ca, P, O, C, Au and Na[43].

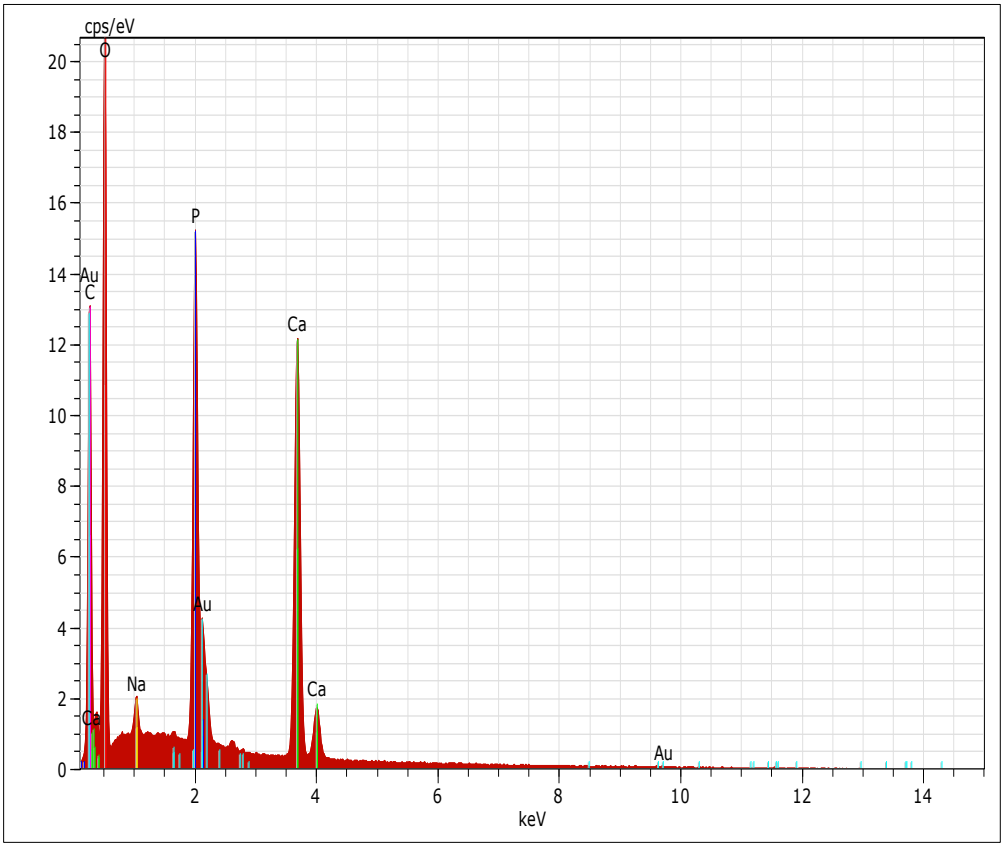

Figure 14: Elemental analysis of 1 cycle hydroxyapatite coated knitted silk scaffold

5.1.2.4.2 Elemental analysis of 3 cycles Hap soaked knitted silk scaffold

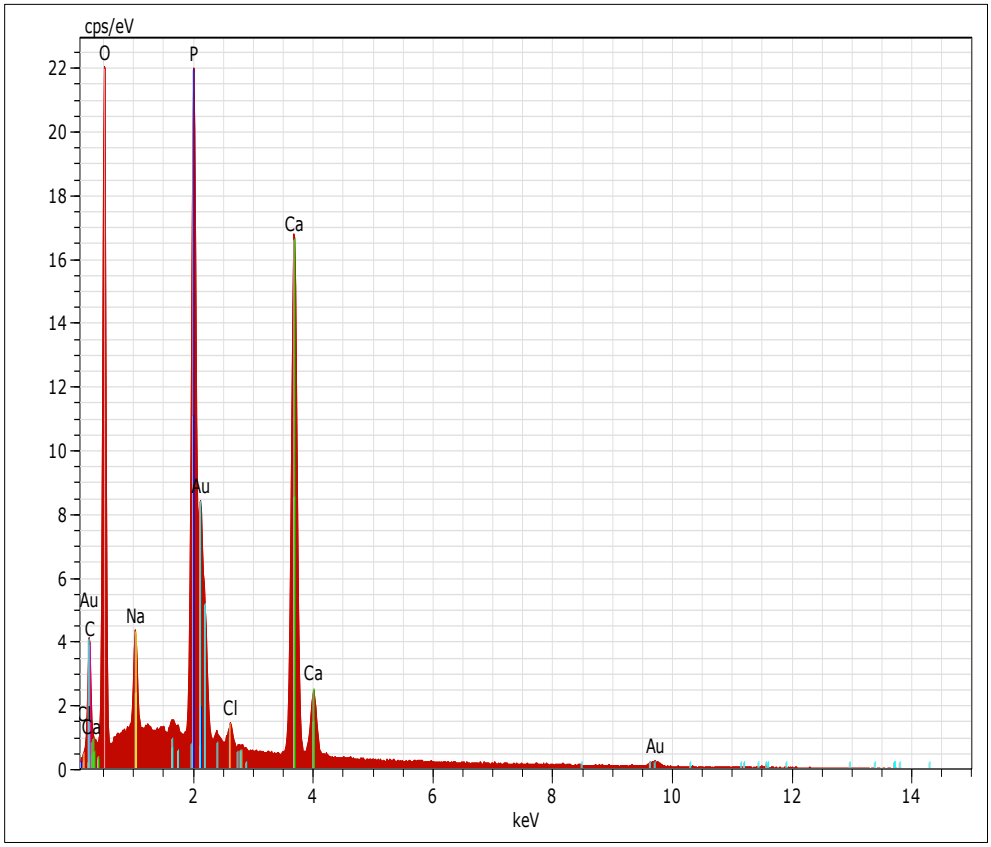

Figure 15: Elemental Analysis of 3 cycle hydroxyapatite coated knitted silk scaffold

5.1.3 Morphology of Silk/Chitosan coated knitted scaffold

Silk/Chitosan coated scaffold was prepared by preparing a solution containing mixture of equal concentrations of both silk and chitosan, and subjecting the solution to freeze drying. Freeze drying facilitates the evaporation of the volatile content of the solution by first freezing it and lowering the pressure down to vacuum conditions, in turn converting the solid solvent directly into vapour, in a process known as sublimation.

Silk/Chitosan layered over knitted silk scaffold appeared as smooth sponges once the solvent was removed. Depending on the concentration of silk/scaffold in their respective solutions, the colour of the solution varied from brownish yellow for 2% solution of both silk and

chitosan mixed together; to blackish brown in solution containing 8% of both silk and chitosan. Since the sponges were smooth in nature, the hardness of the material did not vary much with increasing concentration of the individual components[44].

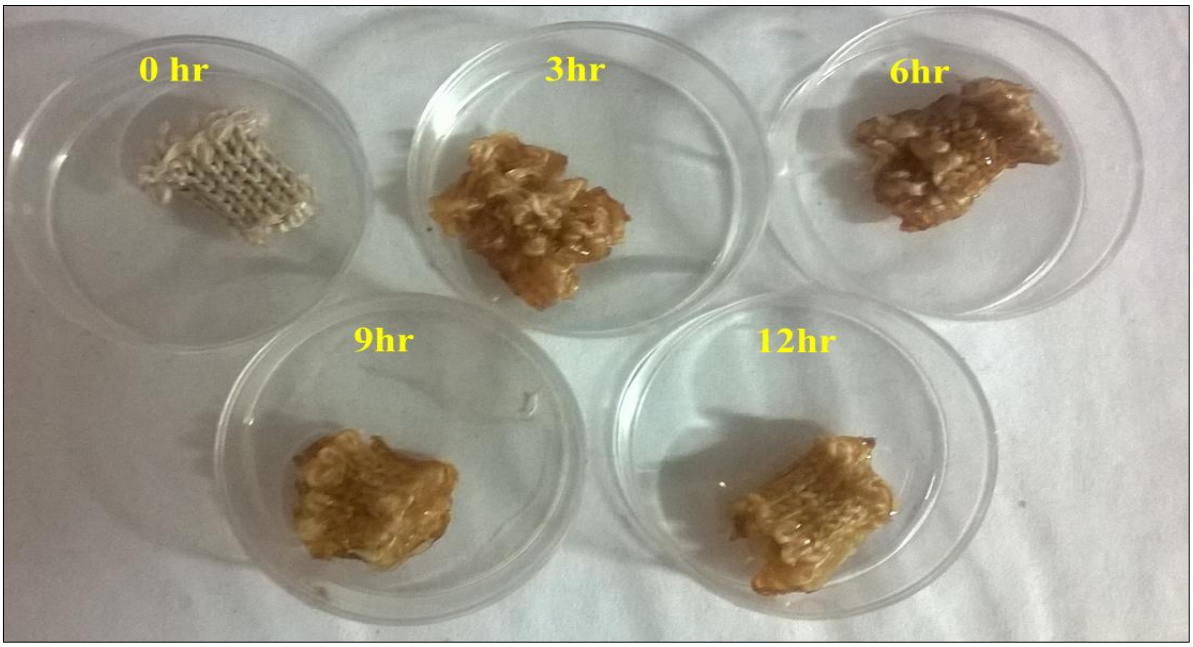

Figure 16: Coating of the silk/chitosan solution on knitted silk scaffold at different time intervals 0, 3, 6,9 and 12 h

5.1.3.1 SEM Analysis of Silk/chitosan coated knitted scaffold

SEM analysis gives the information about the presence of silk/chitosan coating on the surface of the knitted silk scaffold. With increase in time period the coating of polymer solution becomes thickened. FE-SEM analysis revealed the topology of the silk/chitosan coated knitted scaffold

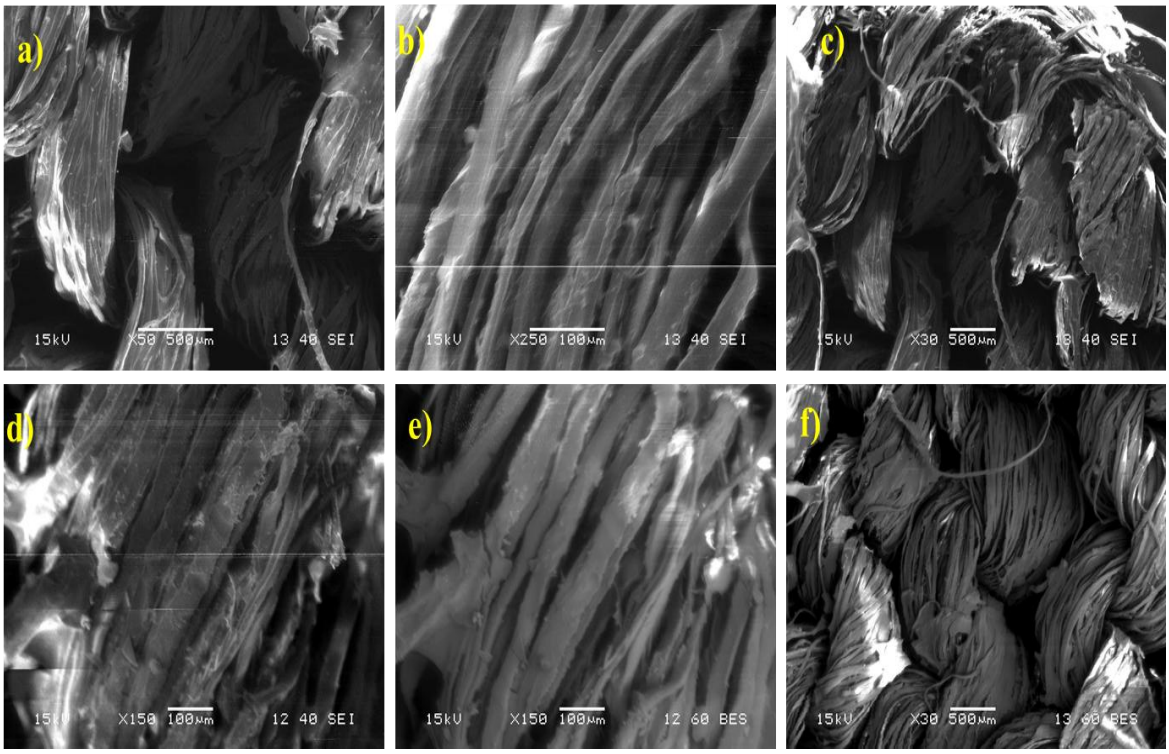

Figure 17: FE-SEM analysis of Silk/chitosan coated knitted silk scaffold

5.1.3.2 XRD of Silk/Chitosan coated knitted scaffold

The XRD peak of silk/chitosan sponge showed aberrant disturbances in peaks indicating that the sponge was majorly constituted of amorphous deposits with low crystallinity. A broad peak was observed around 22º is indicative of chitosan particles and that of 30º indicates presence of silk[45].

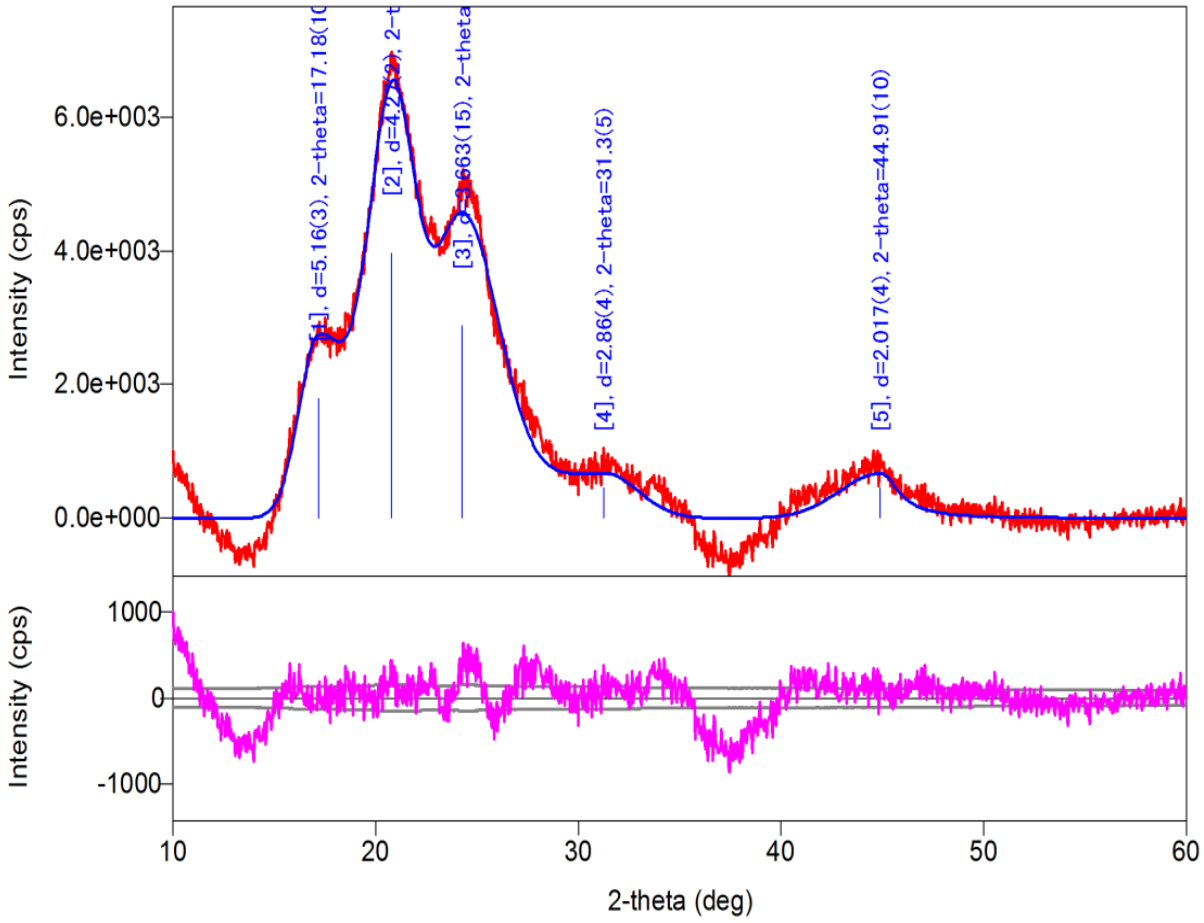

Figure 18: XRD analysis of Silk/chitosan coated knitted silk scaffold

5.1.3.3 FTIR Analysis of Silk/chitosan coated knitted scaffold

FTIR analysis was carried out to determine the bond characteristics and the side chains present in the sample. The major peak at around 1250 cm^{-1} is indicative of the presence of amide III linkage of silk fibroin. The peaks around 2922 cm^{-1} and 1380 cm^{-1} are indicative of amine group of chitosan. Peak around 3444 cm^{-1} indicative of OH^- group of chitosan[46].

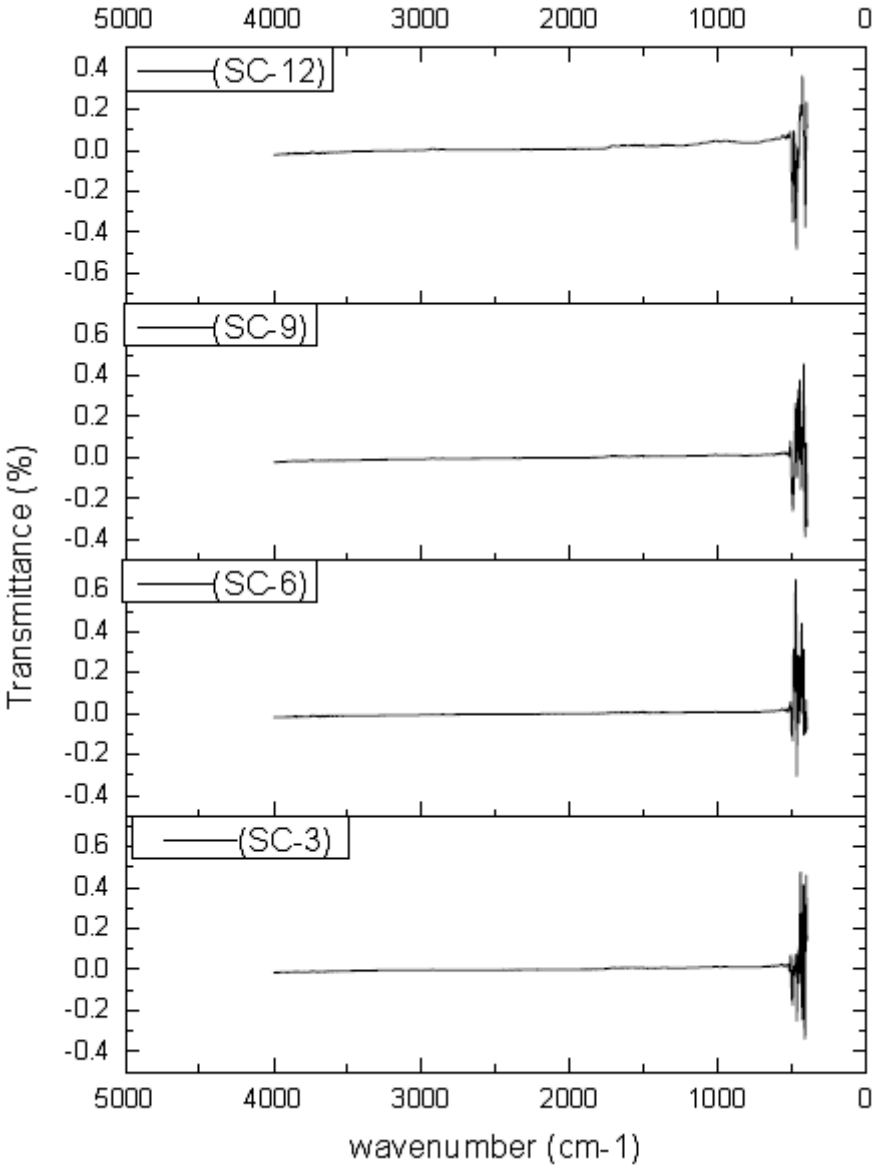

Figure 19: FTIR Spectra of Silk/Chitosan Coated Knitted Silk scaffold

5.1.3.4 EDAX of Silk/chitosan coated knitted silk scaffold

EDX is used for the elemental analysis of the silk/chitosan coated knitted silk scaffold. It gives peaks at different wavelength showing different elements in the sample. According to this graph Different peaks are observed for elements like carbon(C), oxygen(O), nitrogen(N) at different wavelength for the silk/chitosan coated knitted silk scaffold[47].

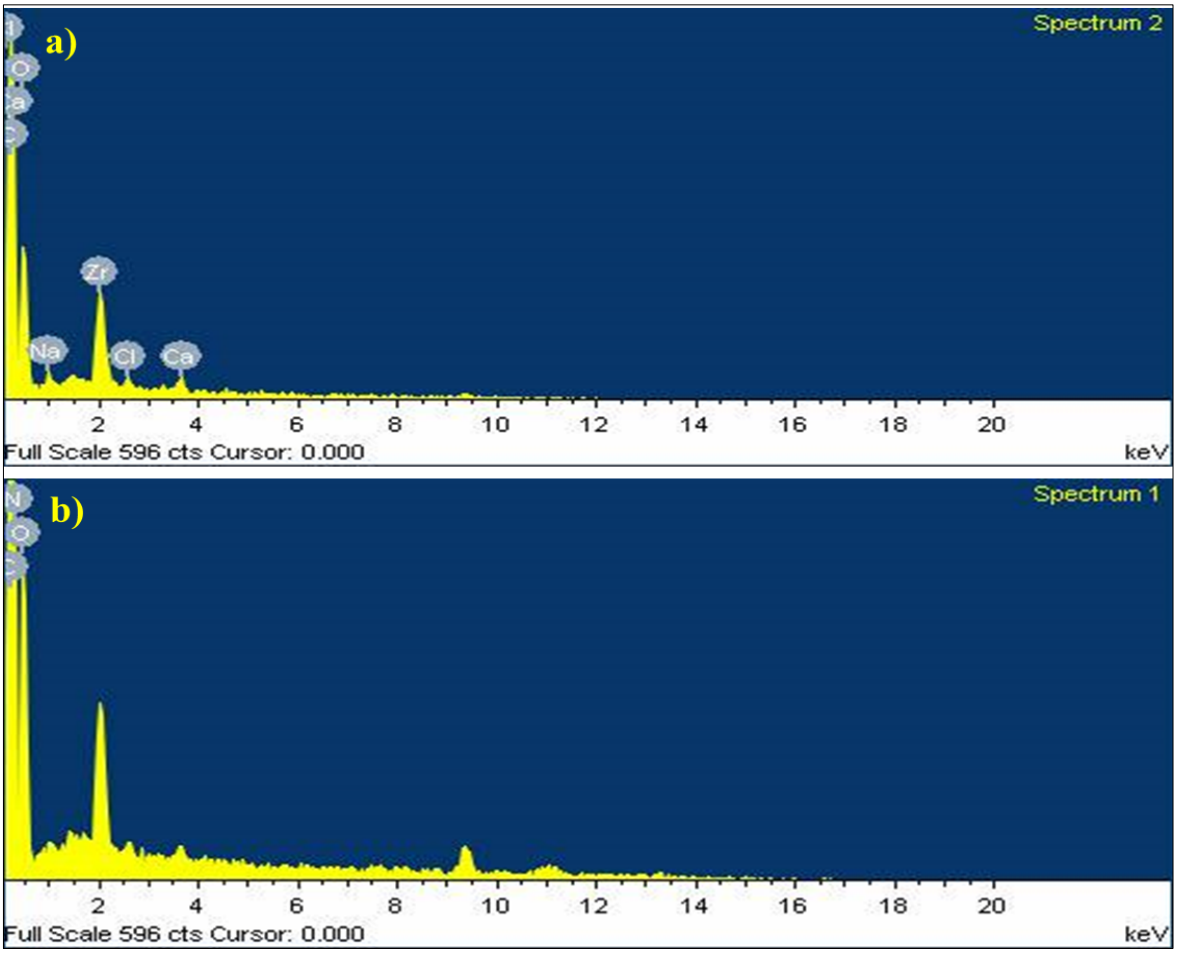

Figure 20: Elemental Analysis of silk/chitosan coated knitted silk scaffold

5.2 MECHANICAL STRENGTH TESTING

The ultimate tensile strength of the knitted silk scaffold was carried out by observing the breaking load of the scaffold. Since the knitted silk forms the base and mechanical support structure for the entire scaffold, the testing of this structure alone was assumed as sufficient to provide an average idea of the strength of the final scaffold with the application of polymer coating. The mechanical strength testing was carried out as an exercise to determine the average degradation rate of the scaffold in body fluids. For this purpose, the knitted silk fibers were immersed in PBS solution prepared at pH 7 and maintained at body temperature . After the stipulated time which was assigned to each scaffold, they were subjected to tensile strength testing.

It was observed that as a thumb of rule, the longer the scaffold was immersed in PBS, the weaker its structure became. The breaking force of the dry scaffold which was not immersed in the buffer solution was found to be at an average of 44 ± 0.2 MPa. The decrease in strength of the scaffold with time was almost linear. Within a week the ultimate breaking force of the knitted silk fibres were observed to be 39 ± 0.61 MPa. At the end of the experimental period at 30 days, the strength of the scaffold had decreased to an average of 29.5 ± 0.53 MPa. This study shows that the scaffold lost its strength almost 33% over a period of 30 days. The strength of the material is assumed to increase marginally with the addition of polymer materials such as Hydroxyapatite and Silk/Chitosan[46].

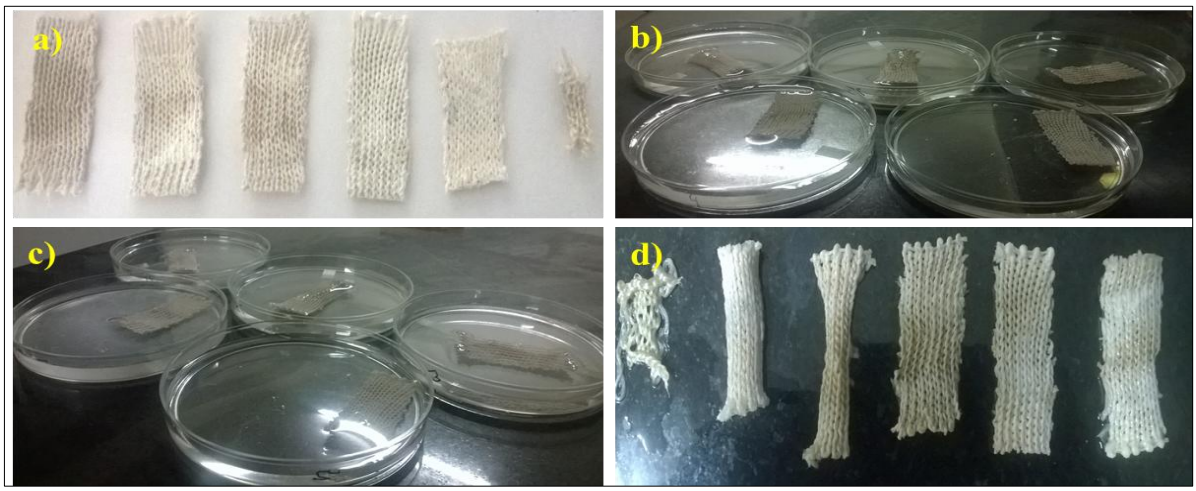

Figure 21: Hydroxyapatite coated knitted silk scaffold dipped in a PBS for Degradability study

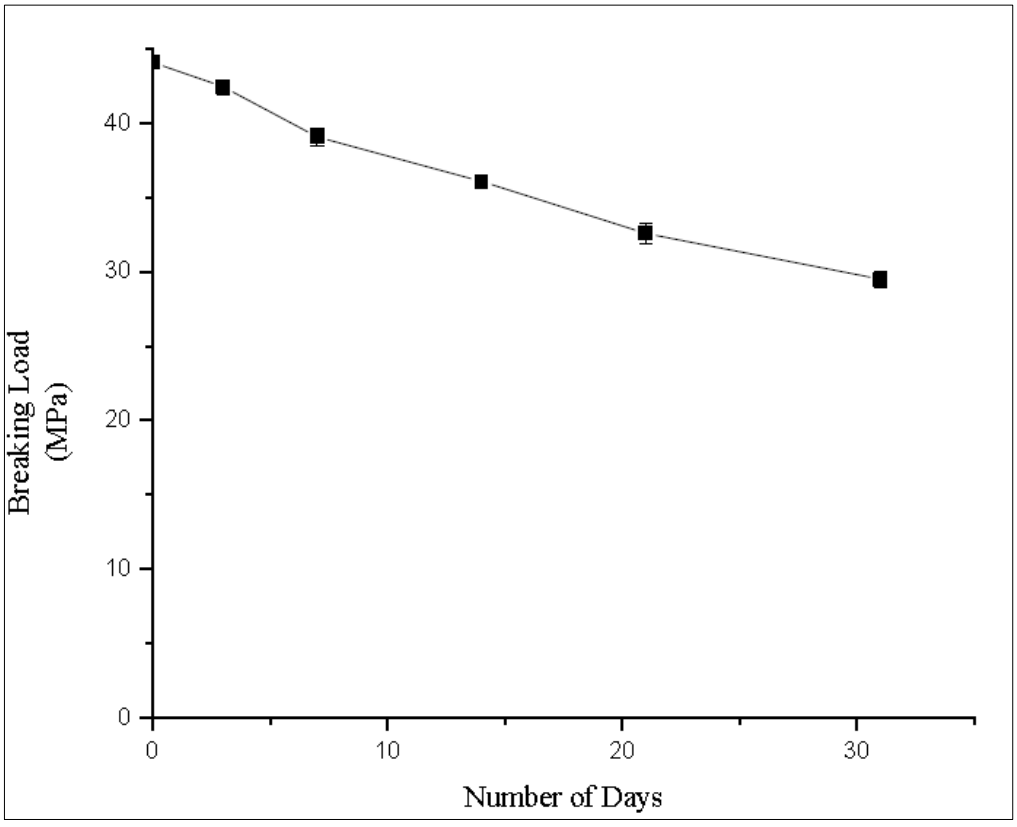

Figure 22: Mechanical strength testing of HA coated knitted silk based scaffold immersed in PBS over a period of time to analyze the degradation of the scaffold

5.3 WATER ABSORPTION STUDIES

The study was carried out to learn the water absorption capability and capacity of the knitted silk scaffold layered with different polymer coatings. The scaffolds were immersed in PBS solution at 37ºC and observed for changed in weight for an interval of 60 minutes until there was so concurrent change in scaffold wet weight observed. The difference between the final and initial weights of the scaffold gave an interpretation of the water absorption capacity of the scaffold.

5.3.1 Water Absorption Study for Hydroxyapatite coated knitted silk scaffold

The hydroxyapatite coated portion of the knitted silk scaffold was found to possess least capability for water absorption. Over a period of 360 minutes, the hydroxyapatite-knitted silk scaffold was able to absorb a total of 74.5% of its weight of PBS, which was attained by the scaffold which had undergone 2 cycles of alternate soaking process for hydroxyapatite layering. Even with increasing water absorption in the beginning, the values suddenly declined as the number of alternate soaking process incremented. It was also observed that all the scaffolds equally absorbed water within a duration of 200 minutes further to which there was minimal change in absorption. Owing to its maximum absorption capacity, this variant of alternate soaking process was used to carry out further studies over the scaffold[40].

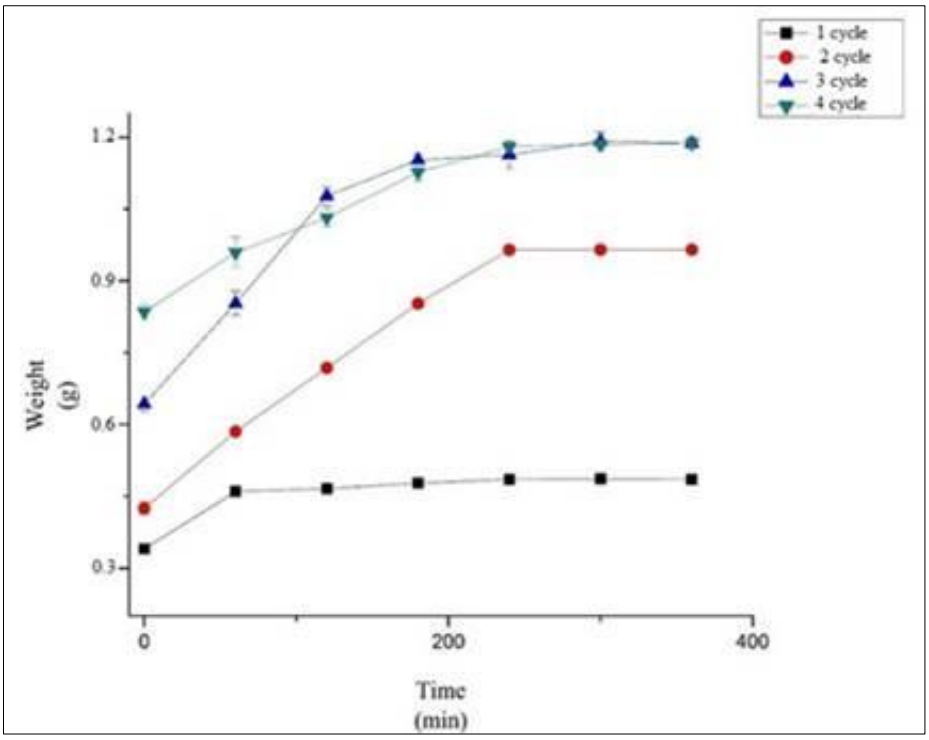

Figure 23: Water absorption study of 4 cycles Hydroxyapatite soaked knitted silk scaffold

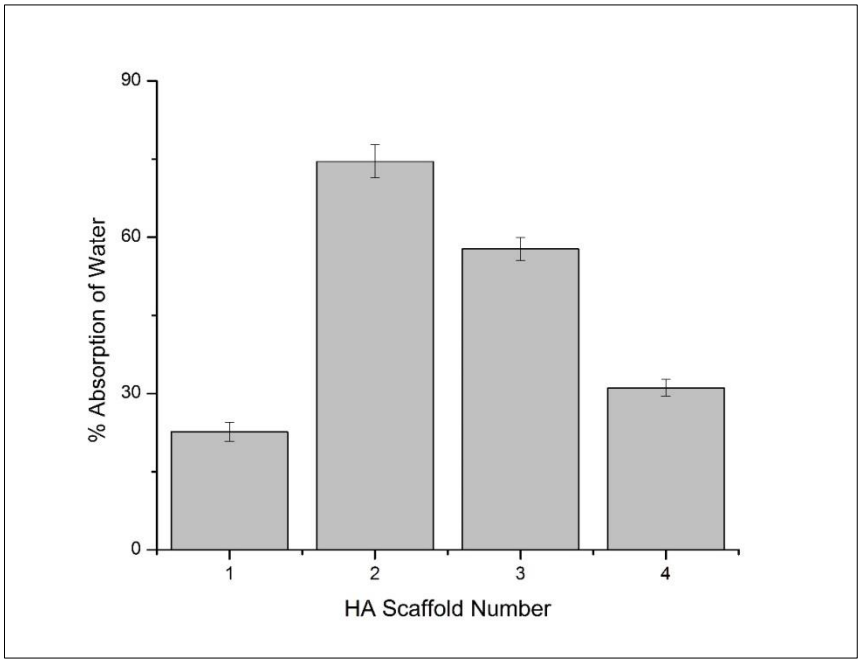

Figure 24: Percentage of Water absorption by hydroxyapatite soaked knitted silk scaffold

5.3.2 Water Absorption Study for Silk/Chitosan coated knitted silk scaffold

The percentage of water absorbed was found to be highest for the scaffold with 2% silk/chitosan concentration, with its final weight increasing almost 400% that of its initial dry weight at the end of 300 minutes. It was observed that with the increasing concentration of silk/chitosan, the sponge also tended to turn brittle when immersed in water and started dislodging itself from the knitted silk mesh. The uptake of water by the sponges was uniform and linear with the increase in concentration of silk/chitosan. The saturation point of the water absorption was reached at around 250 minutes further to which there was no significant absorption of water observed. Based on this study it was concluded that 2% silk/chitosan sponges was the ideal candidate for the final scaffold[48].

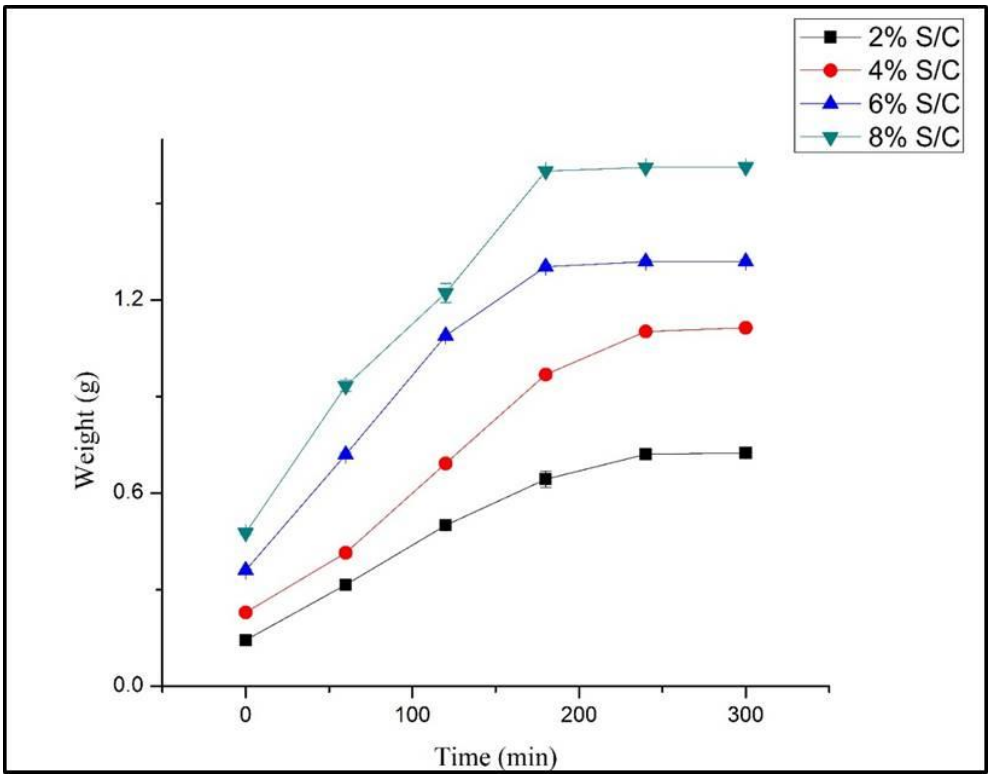

Figure 25: Water absorption study of Silk/chitosan coated knitted silk scaffold

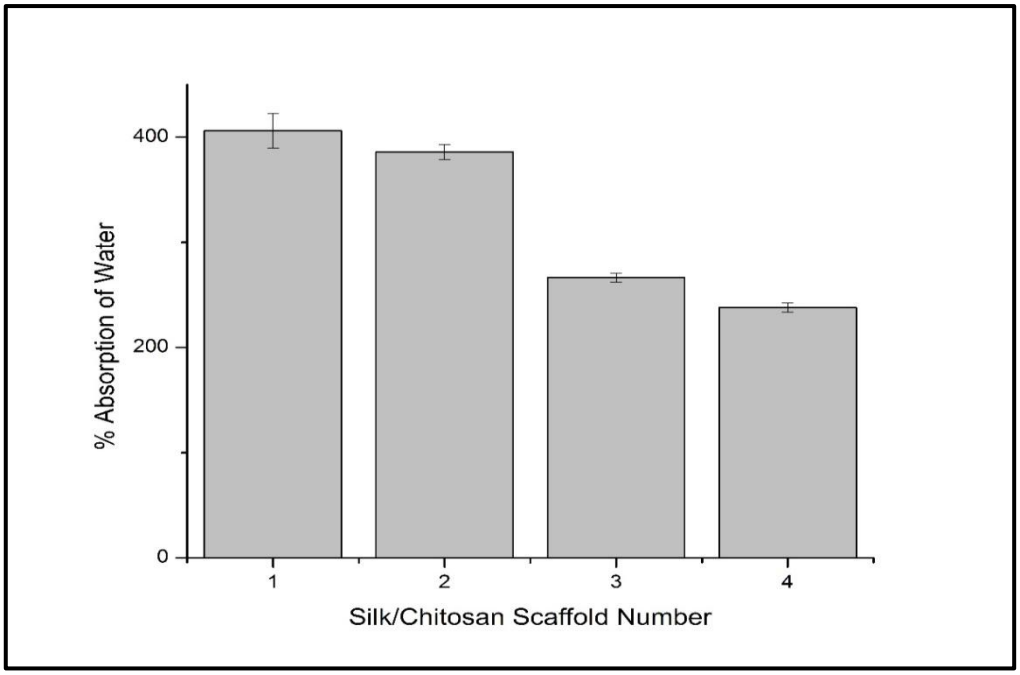

Figure 26: Percentage of water absorption by silk/chitosan coated knitted silk

5.4 CELL CULTURE AND *IN VITRO* - BIOCOMPATIBILITY STUDIES

5.4.1 Cell Culture Studies:

We cultured Adipose derived stem cells initially cell are less according to the increase in no. of days these cells are proliferate and confluent on 10 days visualize under Fluorescence microscope and these are further used for enthesis compartment[49].

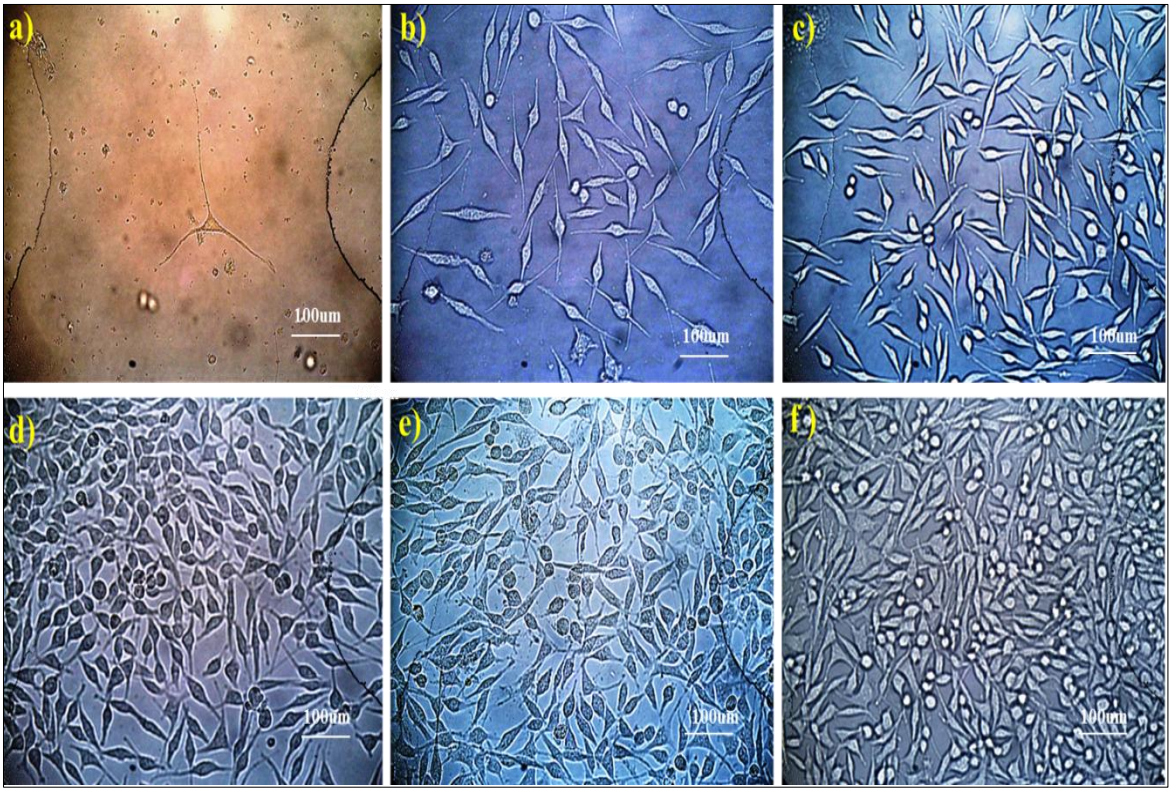

Figure 27: Adipose derived stems Cells after a) 0 days b) 2 days c) 4 days d) 6 days e) 8 days f) 10 days under inverted fluorescence microscope at 40 X magnification

5.4.1.1 MG 63 Cells

Initially we cultured the MG63 (NCCS Pune) cells having concentration on 0 day is 2.8 $X10^5$ Cells/ml on increasing the no. of days after 7 day these cells are confluent up to 9.7 $X10^5$ cells/ml. Then these cells are further used for proliferation studies for bone compartment [50].

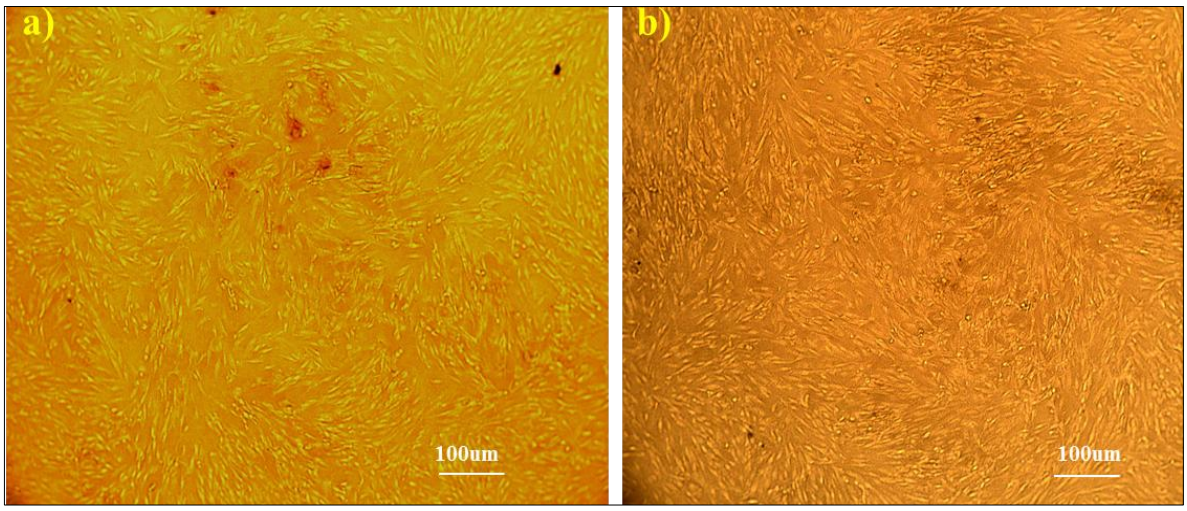

Figure 28: Cultured MG-63 Cells after a) 5 days b) 10 days under inverted fluorescence microscope at10X magnification

5.4.1.2 Saos-2 Cells

Initially we cultured the Saos-2(NCCS Pune) cells having concentration on 0 day is 2.6 $X10^5$ Cells/ml on increasing the no. of days after 7 day these cells are confluent upto 9.1$X10^5$ cells/ml. Then these cells are further used for proliferation studies for Ligament compartment[51].

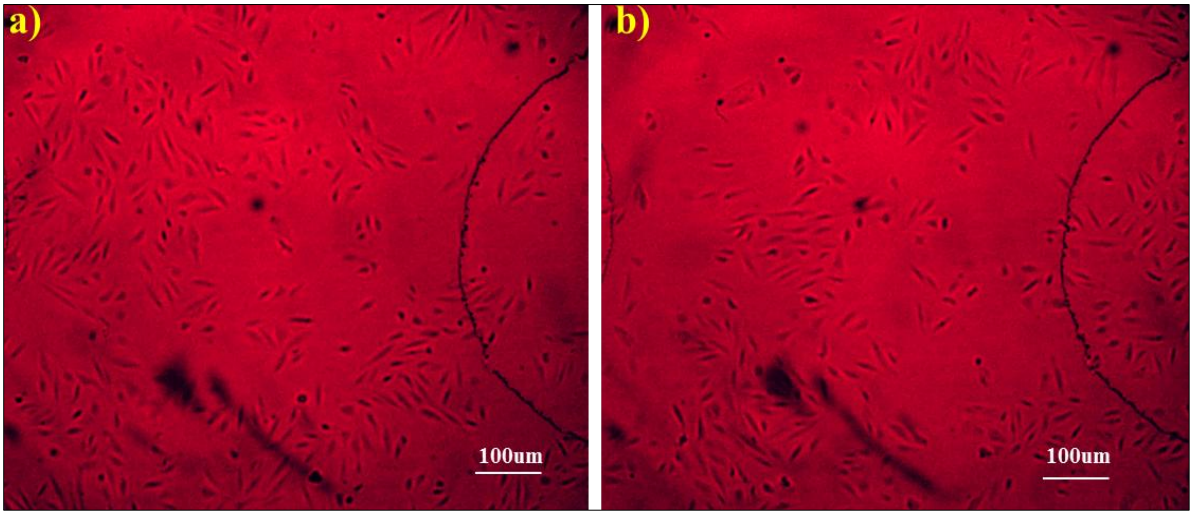

Figure 29: Cultured Saos-2 cells after a) 5days and b) 10 days under inverted fluorescence microscope at 10X magnification

5.4.2 *In vitro*-Biocompatibility studies:

5.4.2.1 Cell adhesion study of Hydroxyapatite coated and SilK/chitosan knitted silk scaffold

Cell adhesion study was carried out by measuring the number of cells that remain in the growth media unattached to the surface of the scaffold. MG-63 osteoblasts were seeded on the hydroxyapatite coated scaffold while Saos-2 fibroblasts were seeded on silk/chitosan scaffolds to measure the efficiency of adhesion of cells. With an initial seeding density of 2.8 X 10^6 cells/ml (MG-63) and 2.3 X 10^6 cells/ml (Saos-2), the study was carried out for 24 hours subsequent to which the scaffolds were removed from the media and the unattached cells remaining in the media and those adhered to the petri dish were counted.

The cell adhesion capacity was found to be 93.3 ± 0.42 % efficient for MG-63 on hydroxyapatite coated scaffold; 92.4 ± 0.96 % efficient for Saos-2 cells seeded on silk/chitosan scaffold. The high efficiency of osteoblast adherence to hydroxyapatite coated scaffold was related to the previously established osteoconductive properties of the mineral. Similar correlation was drawn on the attachment efficiency of fibroblasts on silk/chitosan coated scaffold[52].

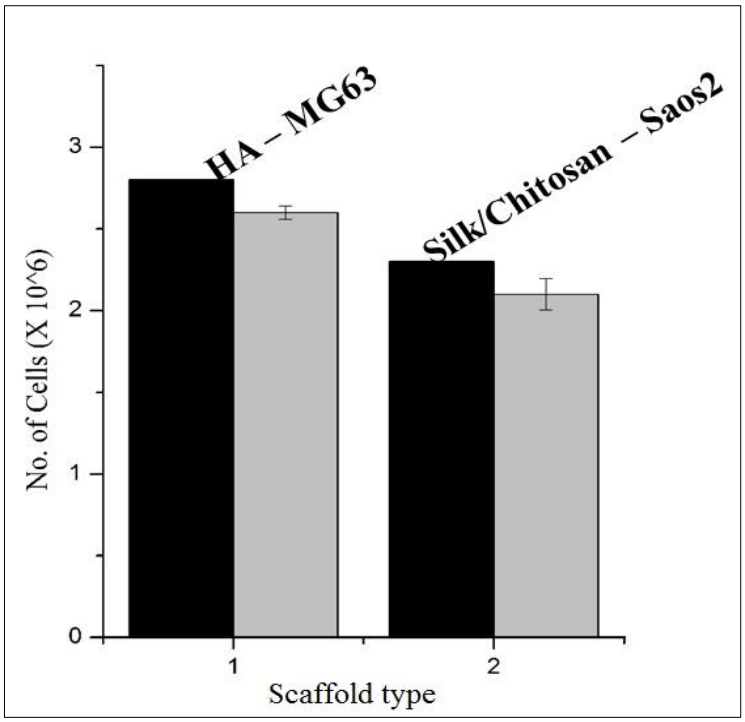

Figure 30: Cell adhesion studies of MG-63 on HA soaked Knitted Silk scaffold and Saos-2 on Silk/chitosan coated knitted silk scaffold

5.4.2.2 Cell Proliferation study

MTT assay was carried out to study the proliferation rate of the cells on scaffolds. The assay gave a conclusive indication of the biocompatibility of the scaffold. An initial seed of 1.2 X 10^5 cells/ml (MG-63) was seeded on hydroxyapatite coated scaffold and equal seed concentration of 1.6 X 10^5 cells/ml (Saos-2) was seeded on silk/chitosan scaffold. At the end of 3 days, the cell density was found to be 2.6 X 10^5 cells/ml for MG-63 and 3.1 X 10^5 cells/ml for Saos-2 on silk/chitosan scaffold. At the end of 7 days, the number of osteoblasts on the hydroxyapatite scaffold had increased to 9.1 X 10^5 cells/ml while the number of fibroblast cells on silk/chitosan had increased to 9.4 X 10^5 cells/ml.

The assay determined that alternate soaking process for the coating of hydroxyapatite on knitted silk scaffold was a favourable method for osteoconduction. It also showcases that for similar kind of cells and equal seeding density, silk/chitosan coating on the scaffold was

biocompatible and favoured cell growth. It was also proved that all the two coatings performed on knitted silk scaffold were successful in providing the micro environmental conditions for cell growth and proliferation[53].

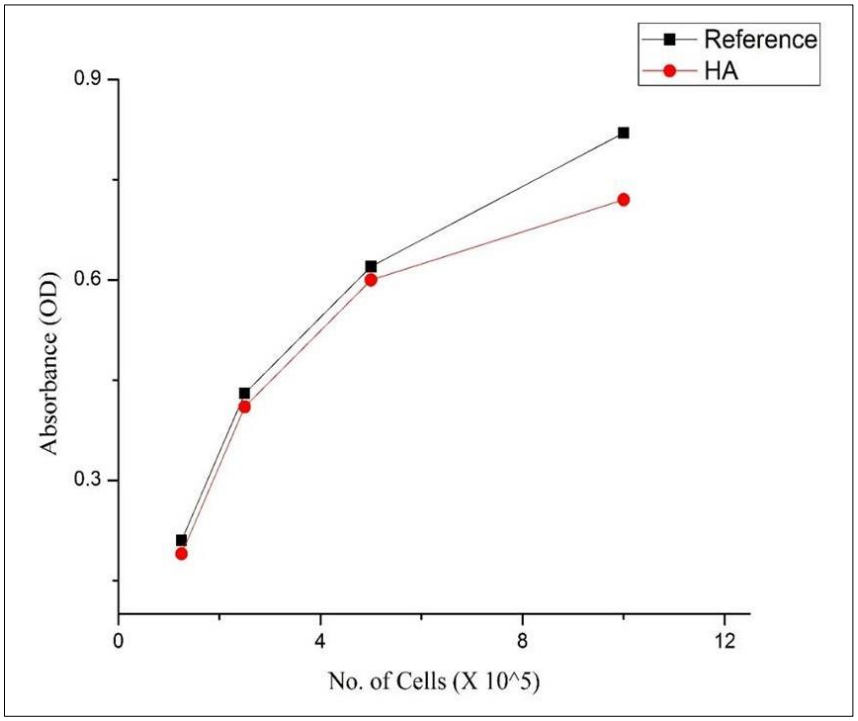

Figure 31: MTT assay to study proliferation of MG-63 on HA soaked knitted silk scaffold

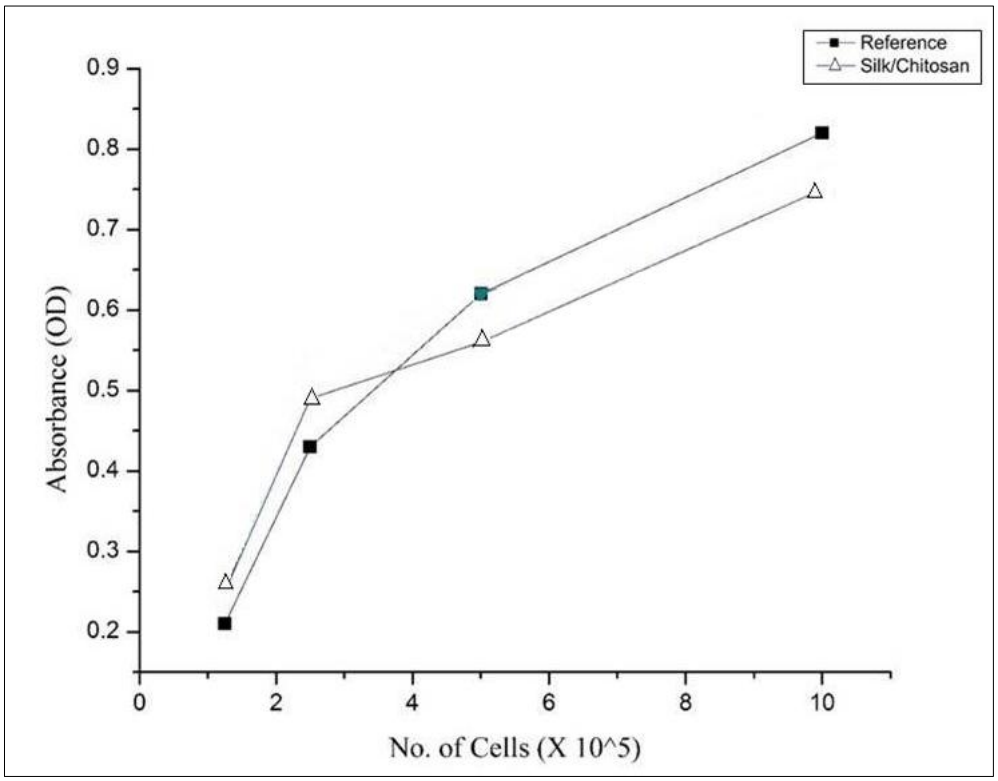

Figure 32: MTT Assay to study proliferation of Saos-2 on silk/chitosan Coated knitted silk scaffold

5.4.2.3 5.4.2.3 Cells Proliferation visualization using Inverted Fluorescence Microscope

After Cell seeding on Knitted Silk scaffold at 0,7,14,21 days we use dye called phallodin dye mixed with the seeded cells and see under Optika inverted Fluorescence microscope which shows the cytoskeleton of the cells through this we can analyse the viability of the seeded cells .and we can also see the change in morphology of the seeded cells on knitted scaffold with increasing days at 0 days cells are round in forms are not attached on the scaffold but on 7 day the cells population is increased and we can see some cells are adhered and change its morphology looks like Fibroblast cells. Finally at the 21 day these cells are fully confluent and all cells are adhered and changed in morphology further these cells are differentiated into other cells.

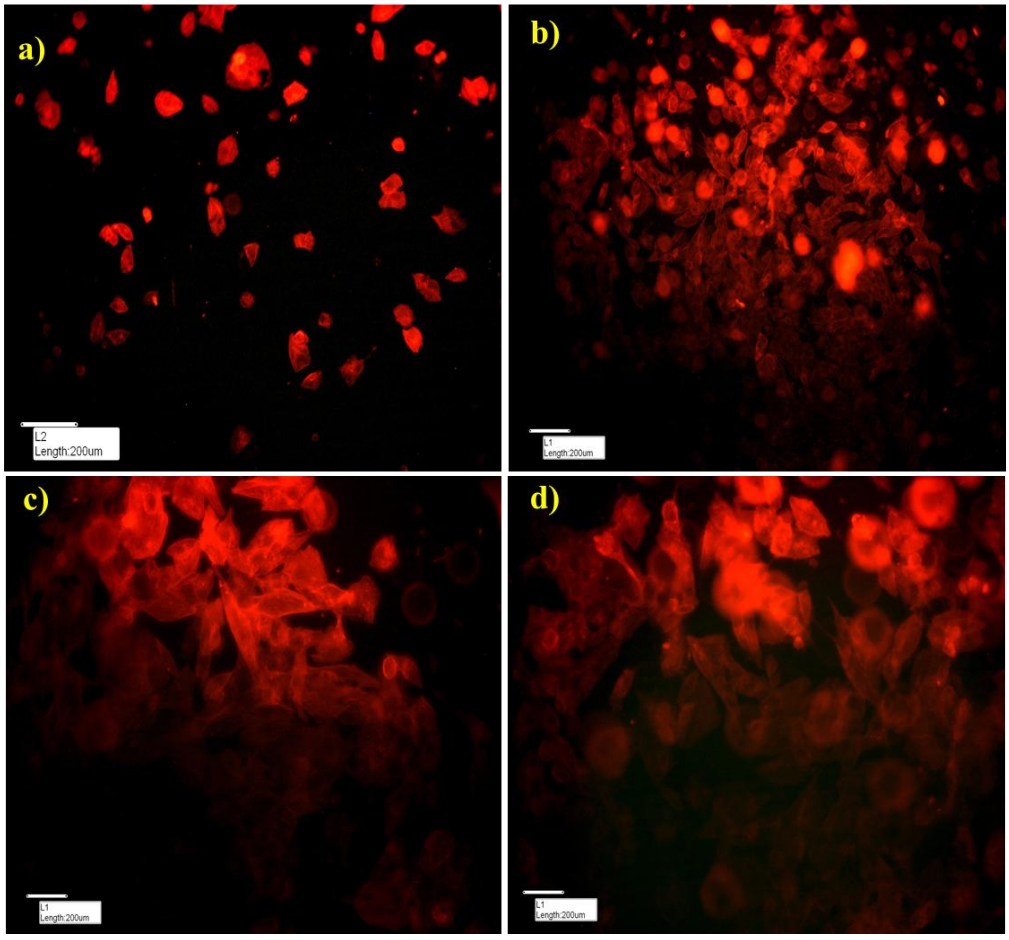

Figure 33: Saos-2 Fibroblast cells are Seeded on coated knitted silk scaffold for a) 0days b)7days c)14 days d)21 days visualized under Inverted fluorescence microscope

CHAPTER-6

CONCLUSION

6 CONCLUSION

The anterior cruciate ligament is one of the most crucial ligaments of the body with one of the highest cases of injury related maladies of the organ. Out of the several methods that are available, tissue engineering is the best sought out method for the rectification of the injury. However, the tissue engineering experiments are not usually successful because of the failure of the ligament to integrate to the bone and form a firm bond, due to which the result is that the organ either usually fails to grow, or integrate and hence slips off, or both. Due to these problems there has been a large number of study to resolve this problem. The current study had focused on fabrication of a knitted silk based scaffold for the growth of not only ligament but also the associated tissues such as fibro cartilaginous enthesis and bone so that the integration of the bone to the ligament is an easy process. The scaffold that was fabricated was a multi-compartmental knitted silk mesh on which coatings of biopolymers were applied. For the efficient growth of cells, hydroxyapatite was coated to help growth of osteoblasts, silk/chitosan was overlaid for the growth of enthesis tissue and gelatin was incorporated for the growth of ligament cells or stem cells which will differentiate into ligament cells. Various methods were employed in the coating of these polymers such as alternate soaking technique, freeze drying and plain coating. A number of studies such as biocompatibility, water absorption, mechanical strength and morphological characterization were carried out on the coatings to prove them as good candidates for the growth and proliferation of cells. The results showed that the coatings had good water absorption, good mechanical strength provided by the knitted silk mesh and satisfactorily biocompatible to validate the scaffold as a good source to implant bone-ligament-bone tissue grafts.

REFERENCES

[1] B. P. Boden, G. S. Dean, J. A. Feagin Jr, and W. E. Garrett Jr, "Mechanisms of anterior cruciate ligament injury," *Orthopedics,* vol. 23, pp. 573-578, 2000.

[2] J. Z. Paxton, K. Baar, and L. M. Grover, "Current progress in enthesis repair: Strategies for interfacial tissue engineering," *Orthopedic & Muscular System: Current Research,* 2012.

[3] F. Noyes, D. Butler, E. Grood, R. Zernicke, and M. Hefzy, "Biomechanical analysis of human ligament grafts used in knee-ligament repairs and reconstructions," *The Journal of Bone & Joint Surgery,* vol. 66, pp. 344-352, 1984.

[4] A. Caraffa, G. Cerulli, M. Projetti, G. Aisa, and A. Rizzo, "Prevention of anterior cruciate ligament injuries in soccer," *Knee surgery, sports traumatology, arthroscopy,* vol. 4, pp. 19-21, 1996.

[5] C. H. Turner and D. B. Burr, "Basic biomechanical measurements of bone: a tutorial," *Bone,* vol. 14, pp. 595-608, 1993.

[6] T. Hayami, M. Pickarski, G. A. Wesolowski, J. Mclane, A. Bone, J. Destefano, G. A. Rodan, and L. T. Duong, "The role of subchondral bone remodeling in osteoarthritis: reduction of cartilage degeneration and prevention of osteophyte formation by alendronate in the rat anterior cruciate ligament transection model," *Arthritis & Rheumatism,* vol. 50, pp. 1193-1206, 2004.

[7] M. Benjamin, B. Moriggl, E. Brenner, P. Emery, D. McGonagle, and S. Redman, "The "enthesis organ" concept: why enthesopathies may not present as focal insertional disorders," *Arthritis & Rheumatism,* vol. 50, pp. 3306-3313, 2004.

[8] M. Benjamin and J. Ralphs, "Fibrocartilage in tendons and ligaments—an adaptation to compressive load," *Journal of Anatomy,* vol. 193, pp. 481-494, 1998.

[9] J. Du, B. C. Pak, R. Znamirowski, S. Statum, A. Takahashi, C. B. Chung, and G. M. Bydder, "Magic angle effect in magnetic resonance imaging of the Achilles tendon and enthesis," *Magnetic resonance imaging,* vol. 27, pp. 557-564, 2009.

[10] T. R. Oegema, R. J. Carpenter, F. Hofmeister, and R. C. Thompson, "The interaction of the zone of calcified cartilage and subchondral bone in osteoarthritis," *Microscopy research and technique,* vol. 37, pp. 324-332, 1997.

[11] W. Cormick, "Enthesopathy–a personal perspective on its man-ifestations, implications and treatment," *Australasian Journal of Ultrasound in Medicine November,* vol. 13, p. 4, 2010.

[12] K. D. Shelbourne and P. Nitz, "Accelerated rehabilitation after anterior cruciate ligament reconstruction," *The American journal of sports medicine,* vol. 18, pp. 292-299, 1990.

[13] M. Mander, J. Simpson, A. McLellan, D. Walker, J. Goodacre, and W. C. Dick, "Studies with an enthesis index as a method of clinical assessment in ankylosing spondylitis," *Annals of the Rheumatic Diseases,* vol. 46, pp. 197-202, 1987.

[14] F. G. Girgis, J. L. Marshall, and A. A. M. JEM, "The Cruciate Ligaments of the Knee Joint: Anatomical. Functional and Experimental Analysis," *Clinical orthopaedics and related research,* vol. 106, pp. 216-231, 1975.

[15] D. W. Hutmacher, "Scaffolds in tissue engineering bone and cartilage," *Biomaterials,* vol. 21, pp. 2529-2543, 2000.

[16] J. P. Spalazzi, E. Dagher, S. B. Doty, X. E. Guo, S. A. Rodeo, and H. H. Lu, "In vivo evaluation of a multiphased scaffold designed for orthopaedic interface tissue engineering and soft tissue-to-bone integration," *Journal of Biomedical Materials Research Part A,* vol. 86, pp. 1-12, 2008.

[17] A. Seidi, M. Ramalingam, I. Elloumi-Hannachi, S. Ostrovidov, and A. Khademhosseini, "Gradient biomaterials for soft-to-hard interface tissue engineering," *Acta biomaterialia,* vol. 7, pp. 1441-1451, 2011.

[18] K. L. Moffat, W.-H. S. Sun, P. E. Pena, N. O. Chahine, S. B. Doty, G. A. Ateshian, C. T. Hung, and H. H. Lu, "Characterization of the structure–function relationship at the ligament-to-bone interface," *Proceedings of the National Academy of Sciences,* vol. 105, pp. 7947-7952, 2008.

[19] J. A. Cooper, H. H. Lu, F. K. Ko, J. W. Freeman, and C. T. Laurencin, "Fiber-based tissue-engineered scaffold for ligament replacement: design considerations and in vitro evaluation," *Biomaterials,* vol. 26, pp. 1523-1532, 2005.

[20] S. Sahoo, S. L. Toh, and J. C. Goh, "A bFGF-releasing silk/PLGA-based biohybrid scaffold for ligament/tendon tissue engineering using mesenchymal progenitor cells," *Biomaterials,* vol. 31, pp. 2990-2998, 2010.

[21] C. S. Ki, D. H. Baek, K. D. Gang, K. H. Lee, I. C. Um, and Y. H. Park, "Characterization of gelatin nanofiber prepared from gelatin–formic acid solution," *Polymer,* vol. 46, pp. 5094-5102, 2005.

[22] X. Chen, Y.-Y. Qi, L.-L. Wang, Z. Yin, G.-L. Yin, X.-H. Zou, and H.-W. Ouyang, "Ligament regeneration using a knitted silk scaffold combined with collagen matrix," *Biomaterials,* vol. 29, pp. 3683-3692, 2008.

[23] H. Fan, H. Liu, S. L. Toh, and J. C. Goh, "Anterior cruciate ligament regeneration using mesenchymal stem cells and silk scaffold in large animal model," *Biomaterials,* vol. 30, pp. 4967-4977, 2009.

[24] A. A. Green, "The preparation of acetate and phosphate buffer solutions of known pH and ionic strength," *Journal of the American Chemical Society,* vol. 55, pp. 2331-2336, 1933.

[25] S. Sahoo, H. Ouyang, J. C.-H. Goh, T. Tay, and S. Toh, "Characterization of a novel polymeric scaffold for potential application in tendon/ligament tissue engineering," *Tissue engineering,* vol. 12, pp. 91-99, 2006.

[26] H.-J. Jin, S. V. Fridrikh, G. C. Rutledge, and D. L. Kaplan, "Electrospinning Bombyx mori silk with poly (ethylene oxide)," *Biomacromolecules,* vol. 3, pp. 1233-1239, 2002.

[27] T. Furuzono, T. Taguchi, A. Kishida, M. Akashi, and Y. Tamada, "Preparation and characterization of apatite deposited on silk fabric using an alternate soaking process," *Journal of biomedical materials research,* vol. 50, pp. 344-352, 2000.

[28] M. Matsusaki, K. Kadowaki, K. Tateishi, C. Higuchi, W. Ando, D. A. Hart, Y. Tanaka, Y. Take, M. Akashi, and H. Yoshikawa, "Scaffold-Free Tissue-Engineered Construct–Hydroxyapatite Composites Generated by an Alternate Soaking Process: Potential for Repair of Bone Defects," *Tissue Engineering Part A,* vol. 15, pp. 55-63, 2008.

[29] A. Sionkowska and A. Płanecka, "Preparation and characterization of silk fibroin/chitosan composite sponges for tissue engineering," *Journal of Molecular Liquids,* vol. 178, pp. 5-14, 2013.

[30] H. Fan, H. Liu, E. J. Wong, S. L. Toh, and J. C. Goh, "In vivo study of anterior cruciate ligament regeneration using mesenchymal stem cells and silk scaffold," *Biomaterials,* vol. 29, pp. 3324-3337, 2008.

[31] M. Ghiasi, E. Naghashzargar, and D. Semnani, "Silk Fibroin Nano-Coated Textured Silk Yarn by Electrospinning Method for Tendon and Ligament Scaffold Application," in *Nano Hybrids,* 2014, pp. 35-51.

[32] J. P. Spalazzi, S. B. Doty, K. L. Moffat, W. N. Levine, and H. H. Lu, "Development of controlled matrix heterogeneity on a triphasic scaffold for orthopedic interface tissue engineering," *Tissue engineering,* vol. 12, pp. 3497-3508, 2006.

[33] S. Mobini, B. Hoyer, M. Solati-Hashjin, A. Lode, N. Nosoudi, A. Samadikuchaksaraei, and M. Gelinsky, "Fabrication and characterization of regenerated silk scaffolds reinforced with natural silk fibers for bone tissue engineering," *Journal of Biomedical Materials Research Part A,* vol. 101, pp. 2392-2404, 2013.

[34] Y. Zhang, C. Wu, T. Friis, and Y. Xiao, "The osteogenic properties of CaP/silk composite scaffolds," *Biomaterials,* vol. 31, pp. 2848-2856, 2010.

[35] S. Farè, P. Torricelli, G. Giavaresi, S. Bertoldi, A. Alessandrino, T. Villa, M. Fini, M. C. Tanzi, and G. Freddi, "In vitro study on silk fibroin textile structure for Anterior Cruciate Ligament regeneration," *Materials Science and Engineering: C,* vol. 33, pp. 3601-3608, 2013.

[36] J. L. Chen, Z. Yin, W. L. Shen, X. Chen, B. C. Heng, X. H. Zou, and H. W. Ouyang, "Efficacy of hESC-MSCs in knitted silk-collagen scaffold for tendon tissue engineering and their roles," *Biomaterials,* vol. 31, pp. 9438-9451, 2010.

[37] M. V. Berridge and A. S. Tan, "Characterization of the cellular reduction of 3-(4, 5-dimethylthiazol-2-yl)-2, 5-diphenyltetrazolium bromide (MTT): subcellular localization, substrate dependence, and involvement of mitochondrial electron

transport in MTT reduction," *Archives of biochemistry and biophysics,* vol. 303, pp. 474-482, 1993.

[38] H. Liu, H. Fan, S. L. Toh, and J. C. Goh, "A comparison of rabbit mesenchymal stem cells and anterior cruciate ligament fibroblasts responses on combined silk scaffolds," *Biomaterials,* vol. 29, pp. 1443-1453, 2008.

[39] K. Wei, Y. Li, K. O. Kim, Y. Nakagawa, B. S. Kim, K. Abe, G. Q. Chen, and I. S. Kim, "Fabrication of nano-hydroxyapatite on electrospun silk fibroin nanofiber and their effects in osteoblastic behavior," *Journal of Biomedical Materials Research Part A,* vol. 97, pp. 272-280, 2011.

[40] P. He, S. Sahoo, K. S. Ng, K. Chen, S. L. Toh, and J. C. H. Goh, "Enhanced osteoinductivity and osteoconductivity through hydroxyapatite coating of silk-based tissue-engineered ligament scaffold," *Journal of Biomedical Materials Research Part A,* vol. 101, pp. 555-566, 2013.

[41] A. Hamlekhan, F. Moztarzadeh, M. Mozafari, M. Azami, and N. Nezafati, "Preparation of laminated poly (ε-caprolactone)-gelatin-hydroxyapatite nanocomposite scaffold bioengineered via compound techniques for bone substitution," *Biomatter,* vol. 1, pp. 91-101, 2011.

[42] P. He, K. S. Ng, S. L. Toh, and J. C. H. Goh, "In vitro ligament–bone interface regeneration using a trilineage coculture system on a hybrid silk scaffold," *Biomacromolecules,* vol. 13, pp. 2692-2703, 2012.

[43] F. A. Müller, L. Müller, I. Hofmann, P. Greil, M. M. Wenzel, and R. Staudenmaier, "Cellulose-based scaffold materials for cartilage tissue engineering," *Biomaterials,* vol. 27, pp. 3955-3963, 2006.

[44] N. BABU, "Fabrication and Characterization of Knitted Silk-Based Composite Scaffold for Bone-Ligament-Bone (BLB) Graft," National Institute Of Technology Rourkela.

[45] S. Khansari, S. Duzyer, S. Sinha-Ray, A. Hockenberger, A. Yarin, and B. Pourdeyhimi, "Two-stage desorption-controlled release of fluorescent dye and vitamin from solution-blown and electrospun nanofiber mats containing porogens," *Molecular pharmaceutics,* vol. 10, pp. 4509-4526, 2013.

[46] N. Singh, S. S. Rahatekar, K. K. Koziol, T. S. Ng, A. J. Patil, S. Mann, A. P. Hollander, and W. Kafienah, "Directing chondrogenesis of stem cells with specific blends of cellulose and silk," *Biomacromolecules,* vol. 14, pp. 1287-1298, 2013.

[47] K. Ng, X. Wong, J. Goh, and S. Toh, "Development of a Silk-Chitosan Blend Scaffold for Bone Tissue Engineering," in *13th International Conference on Biomedical Engineering*, 2009, pp. 1381-1384.

[48] V. I. Walters, "Design and Analysis of a Collagenous Anterior Cruciate Ligament Replacement," Virginia Polytechnic Institute and State University, 2011.

[49] J. K. Fraser, M. Zhu, I. Wulur, and Z. Alfonso, "Adipose-derived stem cells," in *Mesenchymal Stem Cells*, ed: Springer, 2008, pp. 59-67.

[50] H.-C. Liu, I.-C. Lee, J.-H. Wang, S.-H. Yang, and T.-H. Young, "Preparation of PLLA membranes with different morphologies for culture of MG-63 Cells," *Biomaterials,* vol. 25, pp. 4047-4056, 2004.

[51] S. B. Rodan, Y. Imai, M. A. Thiede, G. Wesolowski, D. Thompson, Z. Bar-Shavit, S. Shull, K. Mann, and G. A. Rodan, "Characterization of a human osteosarcoma cell line (Saos-2) with osteoblastic properties," *Cancer Research,* vol. 47, pp. 4961-4966, 1987.

[52] N. Bhardwaj and S. C. Kundu, "Silk fibroin protein and chitosan polyelectrolyte complex porous scaffolds for tissue engineering applications," *Carbohydrate Polymers,* vol. 85, pp. 325-333, 2011.

[53] F. A. Sheikh, H. W. Ju, B. M. Moon, O. J. Lee, J. H. Kim, H. J. Park, D. W. Kim, D. K. Kim, J. E. Jang, and G. Khang, "Hybrid scaffolds based on PLGA and silk for bone tissue engineering," *Journal of tissue engineering and regenerative medicine,* 2015.